Structure
Article

The GTPase Cycle of the Chloroplast Import Receptors Toc33/Toc34: Implications from Monomeric and Dimeric Structures

Patrick Koenig,[1] Mislav Oreb,[2,4] Anja Höfle,[2,4] Sabine Kaltofen,[3] Karsten Rippe,[3] Irmgard Sinning,[1] Enrico Schleiff,[2,4] and Ivo Tews[1,*]
[1]Heidelberg University Biochemistry Center, Im Neuenheimer Feld 328, 69120 Heidelberg, Germany
[2]Department of Biology I, VW Research Group, Ludwig-Maximilians-Universität München, Menzinger Strasse 67, 80638 München, Germany
[3]Research Group Genome Organization and Function, Deutsches Krebsforschungszentrum and BIOQUANT, Im Neuenheimer Feld 280, 69120 Heidelberg, Germany
[4]Present address: Cluster of Excellence Macromolecular Complexes, Department of Biosciences, JWGU Frankfurt am Main, Max-von-Laue Strasse 9, 60439 Frankfurt, Germany.
*Correspondence: ivo.tews@bzh.uni-heidelberg.de
DOI 10.1016/j.str.2008.01.008

SUMMARY

Transport of precursor proteins across chloroplast membranes involves the GTPases Toc33/34 and Toc159 at the outer chloroplast envelope. The small GTPase Toc33/34 can homodimerize, but the regulation of this interaction has remained elusive. We show that dimerization is independent of nucleotide loading state, based on crystal structures of dimeric Pisum sativum Toc34 and monomeric Arabidopsis thaliana Toc33. An arginine residue is—in the dimer—positioned to resemble a GAP arginine finger. However, GTPase activation by dimerization is sparse and active site features do not explain catalysis, suggesting that the homodimer requires an additional factor as coGAP. Access to the catalytic center and an unusual switch I movement in the dimeric structure support this finding. Potential binding sites for interactions within the Toc translocon or with precursor proteins can be derived from the structures.

INTRODUCTION

The majority of chloroplast proteins are nuclear encoded and cytosolically synthesized. Over 2000 proteins have to be imported into the organelle (Kleffmann et al., 2006; Leister, 2003). The major import pathway uses a multicomponent translocon, the so-called Toc/Tic complex (translocon at the outer/inner envelope of chloroplasts) (Kessler and Schnell, 2006; Li et al., 2007; Oreb et al., 2006). The Toc translocon contains the two membrane-bound GTPases Toc33/34 and Toc159 (Schleiff et al., 2003), which expose their G domains to the cytosol and recognize and then deliver precursor proteins through the translocation pore Toc75. The Toc75 pores oligomerize, and a stoichiometry of (4–5)3 Toc33/34):(4)3 Toc75):(1)3 Toc159) was determined from isolated Toc core complexes by immunochemical methods (Schleiff et al., 2003). Slightly different stoichiometries were found when analyzing chloroplasts (3:3:1; Kikuchi et al., 2006) or outer envelopes (2:5:1; Vojta et al., 2004). Although these discrepancies are within experimental error, they might also suggest a dynamic composition of the Toc complex. Surprisingly, the requirement for such a stoichiometry is not accounted for in current models of protein translocation (Kessler and Schnell, 2006).

Toc33/34 function is essential because the deletion of both paralogs in the Arabidopsis genome—atTOC33 and atTOC34—is embryo lethal (Constan et al., 2004). Like other GTPases, Toc33/34 possesses five G elements involved in nucleotide binding which are linked to and overlap with the switch I and switch II regions (Bourne et al., 1991). Generally, the switches change conformation during the GTPase cycle, and are thus required for functional readout of the particular GTPase (Sprang, 1997; Vetter and Wittinghofer, 2001). Toc33/34 belongs to the class of TRAFAC (translation factor-related) GTPases and together with Aig GTPases forms the Aig1/Toc34/Toc159-like paraseptin GTPase subfamily (Leipe et al., 2002). The function of Aig GTPases has been linked to self-defense in plants (Reuber and Ausubel, 1996) and to the development of T cells in vertebrates (Nitta and Takahama, 2007). Despite identification of these important functions, biochemical and structural characterizations of Aig GTPases are sparse. Because of the close relation to Toc GTPases, the analysis presented here has implications for this medically relevant GTPase subfamily.

The G domains of Toc33/34 (Kouranov and Schnell, 1997) and Toc159 (Becker et al., 2004; Chen et al., 2000; Ivanova et al., 2004) directly interact with the transit peptide of the precursor protein. For Toc33/34, it has been shown that binding is somewhat stronger when the GTPase is in the GTP-bound state (Gutensohn et al., 2000; Jelic et al., 2003; Schleiff et al., 2002), and precursor protein interaction accelerates GTP hydrolysis moderately (Jelic et al., 2002, 2003; Reddick et al., 2007). Models describing the import of proteins into the chloroplast are based on dimerization events that take place at the translocation pore (Kessler and Schnell, 2004; Li et al., 2007). There is evidence for an interaction between the Toc33/34 and Toc159 GTPases, such as that determined by Toc33/34 affinity chromatography using radioactively labeled (Bauer et al., 2002; Becker et al., 2004; Hiltbrunner et al., 2001; Smith et al., 2002; Wallas et al., 2003) or chemically purified Toc159 as substrate (Becker et al., 2004; Hiltbrunner et al., 2001; Smith et al., 2002; Wallas

Table 1. Crystallographic Analysis

	psToc34$_{GMPPNP}$ (PDB Code: 3BB1)	atToc33$_{GDP}$ (PDB Code: 3BB3)	atToc33$_{GMPPNP}$ (PDB Code: 3BB4)
Data Collection Statistics			
Space group	$P2_12_12$	$P4_12_12$	$P4_12_12$
Unit cell a, b, c (Å)	178.8, 180.1, 90.9	121.6, 121.6, 42.7	121.6, 121.6, 42.7
Number of molecules in asymmetric unit	8	1	1
Mosaicity ( )	0.28	0.27	0.26
Solvent content (%)	54	46	48
Average B (Å^2)	65.4	82	69.8
Unique reflections	72,688	7,234	7,827
Resolution (Å)/HR shell (Å)	50 2.80/2.85 2.80	30 2.94/3.04 2.94	25.0 2.84/2.94 2.84
R_{sym} (%)/HR shell (%)[a]	7.7/47.1	8.1/46.6	8.5/48.6
Completeness (%)/HR shell (%)	99.5/95.9	99.3/97.9	99.6/100.0
<I>/<sI>/HR shell	15.5/2.4	14.4/1.9	15.4/2.2
Redundancy/HR shell	3.8/3.4	6.1/4.2	5.8/6.0
Refinement Statistics			
Amino acids (chain A)	2–196, 202–258	7–67, 71–251	7–67, 72–250
Total protein atoms (including double conformations)	15,842	1,923	1,946
Water	298	24	25
Ligand atoms	GMPPNP, Mg^{2+}, PEG, glycerol	GDP, Mg^{2+}	GMPPNP, Mg^{2+}
Rmsd bonds (Å)	0.018	0.020	0.020
Rmsd angles ( )	2.2	2.1	2.1
R_{free} (%)[b]	28.6	26.2	27.7
R_{work} (%)[c]	22.6	21.8	21.8
Ramachandran plot[d]			
Most favored (residues/%)	1,456/85.5	190/88.8	186/87.7
Additional favored (residues/%)	224/13.2	22/10.3	23/10.8
Generously allowed (residues/%)	22/1.3	2/0.9	2/0.9
Disallowed (residues/%)	1/0.1	0/0	1/0.5

[a] $R_{sym} = S_hS_ij I(h) \quad I(h)_ij/S_hS_iI(h)_i$, where I(h) is the mean intensity.
[b] Five percent of the data were excluded to calculate R_{free}.
[c] $R_{work} = S_hjjF_{obs}(h)j \quad jF_{calc}(h)jj/ShjF_{obs}(h)j$, where $F_{obs}(h)$ and $F_{calc}(h)$ are observed and calculated structure factors, respectively.
[d] Laskowski et al. (1993).

et al., 2003). Furthermore, Toc33/34 has been shown to homodimerize (Jelic et al., 2003; Reddick et al., 2007; Weibel et al., 2003; Yeh et al., 2007). The dimer interface is known from a crystallographic 3D structure of Pisum sativum Toc34 in the GDP-bound state (Sun et al., 2002), but it is unclear whether a Toc34 homodimer is required for regulation of the Toc complex. Also, the synchronization of the GTPase cycle with homodimerization is controversial (Weibel et al., 2003; Yeh et al., 2007). This prompted us to determine the 3D structures of the GMPPNP- and GDP-bound states of Toc33/34 GTPases from Pisum sativum and Arabidopsis thaliana. We derive switch movements during GTP hydrolysis, priming the understanding of GTPase regulation. A hypothesis of possible binding events is given here.

RESULTS

The psToc34 Dimer Is Not Self-Activating

The cytosolic G domain of psToc34 (lacking the C-terminal membrane anchor) was purified mainly in the GDP-bound form after recombinant protein production in Escherichia coli. (Regarding nomenclature, we have studied the homologous GTPases atToc33 from Arabidopsis thaliana and psToc34 from Pisum sativum. The first two italicized letters indicate source organism, followed by GTPase name. Amino acid names are referred to simply by organism, i.e., psGlu73 for Glu73 in psToc34. Toc33/34 without a denominator refers to both atToc33 and psToc34 GTPases.) A nucleotide exchange protocol was established to load the GTPase with GMPPNP, a nonhydrolyzable GTP nucleotide analog. Nucleotide loading states were controlled by HPLC analysis (see Figure S1 in the Supplemental Data available with this article online). psToc34$_{GMPPNP}$ crystallized in an orthorhombic space group (Table 1), whereas previously psToc34$_{GDP}$ crystallized under different conditions in a monoclinic space group (Protein Data Bank [PDB] code: 1H65; Sun et al., 2002). The quaternary arrangement of both psToc34$_{GMPPNP}$ and psToc34$_{GDP}$ is a homodimer, without major structural rearrangements (root-mean-square deviation [rmsd] of 0.7 Å for 245 C_a positions).

In the 3D structure of psToc34$_{GMPPNP}$ (Figure 1A), the nucleotide moieties are located at the dimer interface. Dimerization involves a number of loop regions, some of which are Toc-specific sequence insertions. Among others, the loops carrying G elements G2 and G3 as well as a loop connecting b5 with a5 are in this interface (Figure 1B); also involved in dimerization is the loop connecting b4 with a3 that is part of a larger conserved sequence feature named the conserved box (CB in Figure 1A; Krucken et al., 2004, 2005; Nitta and Takahama, 2007). In Toc33/34, the CB forms a number of central secondary structure elements (in red, Figure 1A), namely b strands b3, and b4 and part of helix a3. From the alignment of five Toc GTPases, along with two additional Aig GTPases, a highly conserved arginine can be seen, with a register shift in the Toc159 proteins. This residue, arginine 133 in psToc34, is necessary for dimer formation (Reddick et al., 2007), and it can thus be predicted that dimerization is a recurrent motif in the Aig GTPase family. Arg133 contacts b- and g-phosphates of GMPPNP in the interacting monomer (Figures 1A and 1B), similar to the contacts of Arg133 to the b-phosphate previously observed for psToc34$_{GDP}$ (Sun et al., 2002). The positioning of Arg133 is reminiscent of an arginine finger described before for GTPase-GAP complexes (Scheffzek et al., 1998).

Comparison between psToc34 in GMPPNP- and GDP-bound states revealed preservation of the dimeric state, suggesting that nucleotide load has little if any effect on dimerization. For a GAP function, we anticipated a higher affinity in the GTP-bound form, concomitant with a drastic increase in GTP hydrolysis by the dimeric GTPase (Scheffzek and Ahmadian, 2005). We therefore determined the influence of the nucleotide loading state on GTPase dimerization in solution, using analytical ultracentrifugation. Freshly prepared psToc34 (mainly loaded with GDP; Figure S1) was subjected to sedimentation velocity runs at a concentration of 50 mM monomer protein. Two species with sedimentation coefficients of 2.6S and 3.5S were separated. These correspond to the monomeric and dimeric forms of the GTPase, as determined from the c(M) distribution. The experimentally determined values are in very good agreement with the sedimentation coefficients of 2.7S and 4.0S for the monomer and dimer calculated from the PDB coordinates with the program HYDRO (Garcia de la Torre et al., 1994). From a quantitative analysis of the sedimentation velocity profiles, the dissociation constant (K_D) of 50 ± 20 mM was calculated for the psToc34$_{GDP}$ dimer (Figure 1C), in agreement with previous data (Reddick et al., 2007). However, protein aging was demonstrated to compromise dimerization properties in the homologous GTPase atToc33 (Yeh et al., 2007). Here we assessed the aging effect for psToc34 to investigate whether dimerization was hampered by the time-intensive nucleotide exchange. We performed an experiment similar to GMPPNP exchange, albeit with excess GDP, and found the dissociation constant to be raised 5-fold (K_D = 0.25 ± 0.05 mM), as compared to freshly prepared psToc34$_{GDP}$. After nucleotide exchange with GMPPNP, the dissociation constant was 0.6 ± 0.1 mM. With this caveat, the experiments still demonstrate that psToc34 is able to dimerize in both nucleotide loading states, with slight preference for dimerization in the GDP-bound form. To determine the effect of oligomerization on hydrolysis rates, we performed single-turnover GTP hydrolysis experiments (Prakash et al., 2000) in the concentration range of 0.013 to 4.5 mM protein, that is, across the stoichiometric point for dimer formation. The increase in enzymatic activity by dimerization is about 1.5-fold (Figure 1D). Thus, our analysis of the isolated psToc34 G domain demonstrates that the dimer is not self-activating, possibly lacking an additional regulatory layer.

A Disordered Switch I in Monomeric atToc33

To examine whether such dimerization behavior is a general feature of Toc33/34 GTPases, we extended the analysis to Arabidopsis Toc33. When we analyzed freshly prepared atToc33 by gel filtration, monomeric and dimeric species are observed, in agreement with previous data (Weibel et al., 2003; Yeh et al., 2007). However, analytical ultracentrifugation with atToc33 under similar conditions as employed for psToc34 revealed exclusively monomeric protein populations (data not shown). Thus, the G domain of atToc33 must exhibit a lower association constant for dimerization than the G domain of psToc34. Applying higher protein concentrations than used for psToc34 in ultracentrifugation with absorbance detection is impractical. Thus, to investigate dimerization and to compare the influence of nucleotide load with atToc33 and psToc34 G domains, a filter binding assay was established (Figure 2A). His-tagged Toc proteins of defined concentration and nucleotide loading state (either GDP or GMPPNP preloaded) were immobilized on a nitrocellulose membrane. After saturation with milk powder, the membranes were incubated with GST-tagged Toc proteins, again of defined concentration and nucleotide loading state (either GDP or GMPPNP preloaded). The bound protein fraction was quantified by GST-specific antibodies, and thus the interaction of the proteins was quantified. With GST protein (i.e., no Toc fusion) as negative control, no signals are detectable under the experimental conditions used (data not shown). Although this technique has some limitations, such as mutual steric hindrance or incorrect orientations of immobilized proteins, it is still suitable for a comparative analysis of the nucleotide dependence of dimerization because the mentioned effects are statistically equally distributed. We find that both atToc33 and psToc34 dimerize, and further show a similar nucleotide dependence with a preference for dimerization of the GDP species (Figure 2B). Filter binding data for psToc34 agree with the analytical ultracentrifugation data (Figure 1C). Thus, the small influence of nucleotides on the dimerization as seen for atToc33 and psToc34 might also occur in other Toc33/34 GTPases.

We went on to characterize atToc33$_{GDP}$ and atToc33$_{GMPPNP}$ structurally (Figure 2C; Table 1). Both proteins are monomeric in the crystal structure, which might be explained by the lower association constants of these proteins compared to psToc34. An analysis of crystal contacts (Figure S2) reveals that the largest contact between monomers in the crystal measures approximately 670 Å^2, whereas the dimer interface characterized for psToc34 measures 2750 Å^2 (Sun et al., 2002). Similar to what is observed with psToc34, the structures of atToc33 in different nucleotide loading states are very similar, reflected in an rmsd of 0.36 Å for 239 C_a positions. There is only weak electron density for residues 68–70 in atToc33$_{GDP}$ and for residues 69–71 in atToc33$_{GMPPNP}$. These residues of the switch I region were thus not included in the models. To examine the impact of dimerization on the structure of the GTPase, we compared monomeric atToc33$_{GDP}$ and atToc33$_{GMPPNP}$ with the dimeric psToc34$_{GMPPNP}$ and psToc34$_{GDP}$ structures. All four structures

 All rights reserved

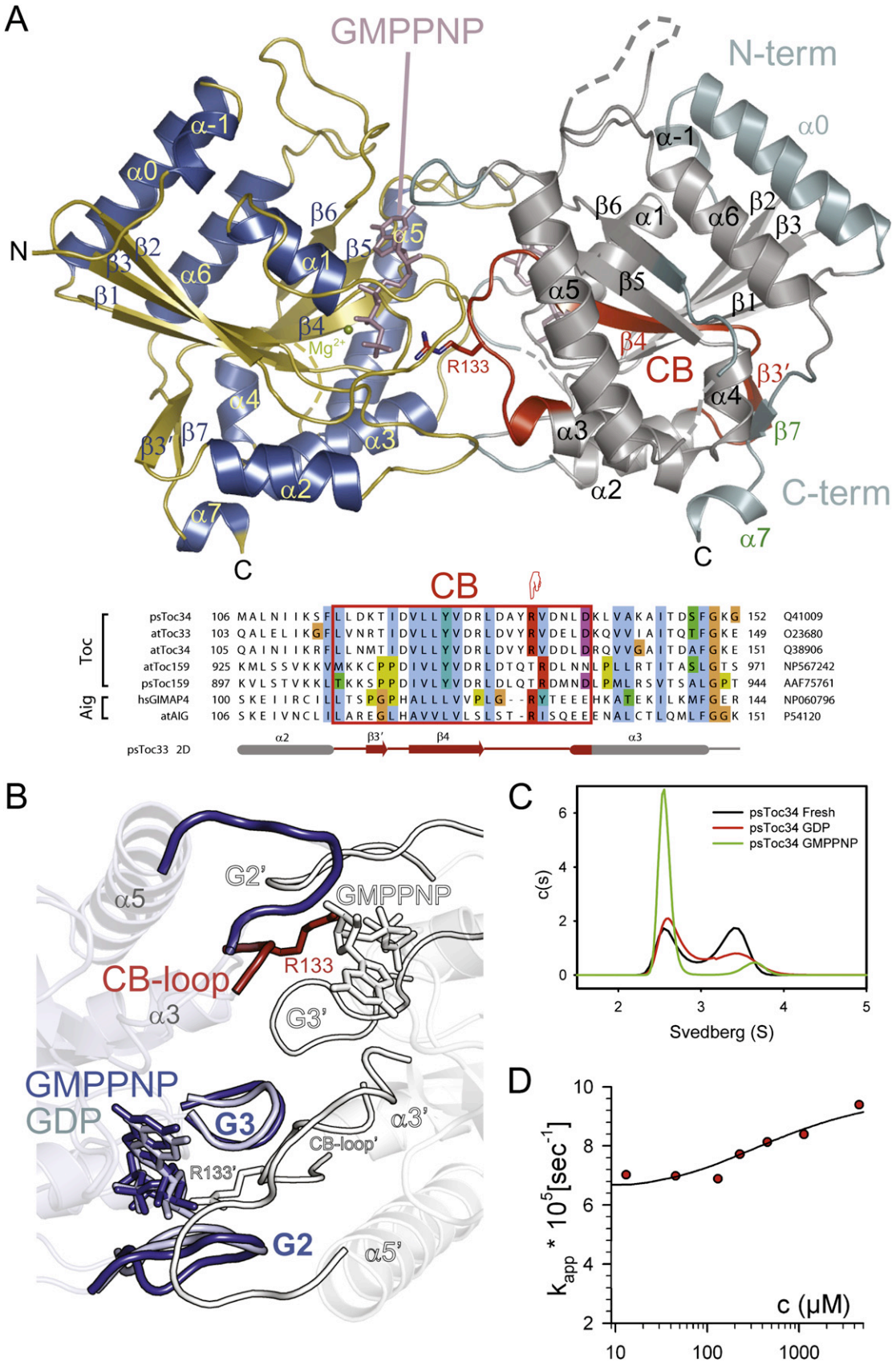
A
GMPPNP
N-term
α-1
α0
β6
α1
α6
β2
β3
α5
β5
N
β3
β2
α6
α1
β5
β1
α5
β5
β1
β4
Mg2+
R133
β4
CB
β3′
α4
α4
β3′
β7
α3
α3
β7
α2
α2
C-term
α7
α7
C
C
CB
Toc
Aig
psToc34 106 MALNIIKSFLLDKTIDVLLYVDRLDAYRVDNLDKLVAKAITDSFGKG 152 Q41009
atToc33 103 QALELIKGFLVNRTIDVLLYVDRLDVYRVDELDKQVVIAITQTFGKE 149 O23680
atToc34 105 QAINIIKRFLLNMTIDVLLYVDRLDVYRVDDLDRQVVGAITDAFGKE 151 Q38906
atToc159 925 KMLSSVKKVMKKCPPDIVLYVDRLDTQTRDLNNLPLLRTITASLGTS 971 NP567242
psToc159 897 KVLSTVKKLTKKSPPDIVLYVDRLDLQTRDMNDLPMLRSVTSALGPT 944 AAF75761
hsGIMAP4 100 SKEIIRCILLTSPGPHALLLVVPLG--RYTEEEHKATEKILKMFGER 144 NP060796
atAIG 106 SKEIVNCLILAREGLHAVVLVLSLST-RISQEEENALCTLQMLFGGK 151 P54120
α2 β3′ β4 α3
psToc33 2D
B
α5
G2′
GMPPNP
CB-loop
R133
α3
G3′
GMPPNP
GDP
G3
α3′
CB-loop′
R133′
G2
α5′
C
psToc34 Fresh
psToc34 GDP
psToc34 GMPPNP
c(s)
Svedberg (S)
D
kapp * 10^5[sec^-1]
c (μM)

are highly similar; e.g. psToc34$_{GMPPNP}$ and atToc33$_{GMPPNP}$ show an rmsd of 0.95 Å for 232 C_a positions. The main difference occurs in the switch I region: not restricted by the dimer contact, switch I in atToc33 is poorly ordered and moved slightly away from the nucleotide binding pocket (Figures 3A and 3B). In dimeric psToc34, switch I is fully resolved and partly stabilized by interaction with the CB and helix a5 in trans (Figures 3C and 3D). Positioning of G2/switch I in psToc34 is maintained by insertion of psPhe70 into a hydrophobic pocket. Although switch II shows a similar conformation in all four structures (Figures 3A–3D), minor movements in this region can be explained by a dimer contact of psTyr102. Restricted switch movement is thus a further characteristic of the two Toc33/34 GTPases atToc33 and psToc34, but even more pronounced in the dimeric form.

Restricted Switch Movement Has Implications for the Catalytic Cycle

Our analysis reveals that the nucleotide load of Toc33/34 has only a minimal influence on dimerization. This is reflected in finite changes observed for the switch regions. We therefore investigated the switch regions in detail to explain this unusual feature for a GTPase. Any significant movement of the G3/switch II region is constrained by a leucine (atLeu95/psLeu97) that enters into a hydrophobic pocket formed by the a2 and a3 helices (Figure 4A). It was predicted that a hydrophobic residue in this region together with a hydrophobic binding pocket could result in the now experimentally confirmed conformation (Mishra et al., 2005). Switch II is fixed in both the GMPPNP- and GDP-bound forms of the GTPase, and moved away from the catalytic center. This is surprising because in other small GTPases, switch II often carries a catalytic residue; in Ras p21, this is the residue Gln61 (Figure 4B; Pai et al., 1990). However, an equivalent to p21-Gln61 is absent in Toc33/34, and hence the classic function of the G3/switch II in the catalytic cycle must be taken over by other protein regions, or by interaction partners.

One of the most obvious candidates is the switch I region of Toc33/34. Although switch I is restricted—partly—by the dimer interface, the region shows above average B factors and retains some conformational flexibility, as seen from a comparison of different protomers in the crystal unit cell (Figure S3). Sequence analysis shows that the catalytic threonine, typical for the small GTPases of the TRAFAC class, is replaced by glutamate (Leipe et al., 2002). Whereas this residue points away from the nucleotide binding pocket in psToc34$_{GMPPNP}$, its carboxyl head group takes the position of g-phosphate in psToc34$_{GDP}$ (Figure 5). In the GDP-bound state, psGlu73 participates in the coordination of the Mg^{2+} ion, as does the g-phosphate in the GMPPNP-bound state (Figure S4). Thus, movement in the switch I region is reduced to a movement of the side chain of Glu73. Because of its role in sensing the nucleotide loading state, we designate residue psGlu73 the nucleotide "tracker." In monomeric atToc33, the equivalent residue atGlu70 does not perform a tracker function: the residue is not resolved in electron density and probably moved away from the nucleotide binding pocket. Therefore, tracking of the nucleotide loading state is of relevance only in the context of the GTPase dimer.

Requirement for a coGAP and Identification of a Putative Protein Binding Site

For GTP hydrolysis to occur, a polar residue is required to position a water molecule for nucleophilic attack on the g-phosphate (Pai et al., 1990; Schweins et al., 1995). In one protomer of psToc34, a water molecule is positioned between the g-phosphate and the backbone carbonyl of switch I psGly74 (Figure 5A). The switch I region might thus play an important role in the intrinsic hydrolysis reaction. Commonly, GTPases are further activated by GAP proteins that stabilize the switch regions and supply additional catalytic residues, often the arginine finger (Scheffzek and Ahmadian, 2005). Structural comparison of the catalytic center of the psToc34 dimer with GTPase-GAP complexes demonstrates that Arg133 in psToc34 in the GMPPNP-bound state is suitably positioned to perform a function as arginine finger (Figure S5). The inability of the dimeric contact to significantly accelerate GTPase activity (Figure 1D) thus points to insufficient stabilization of the catalytic center in the present structures, seen in the remnant flexibility of switch I, or to an absence of a catalytic residue. The GTPase dimer thus requires another factor as coGAP, for example as described for the GTPases Arf and Ran (Goldberg, 1999; Seewald et al., 2003). The coGAP function is required in the GTP-bound state of psToc34; it thus might recognize the tracker glutamate of switch I, leading to stabilization of this region. Interestingly, movement of the tracker glutamate opens up two tunnels in psToc34$_{GMPPNP}$ for direct access to the g-phosphate, only one of which is present in psToc34$_{GDP}$ (Figures 6C and 6D). Hence, no structural rearrangement in the dimer is required for a coGAP that binds and inserts a catalytic residue through one of these holes, whereas the second hole could function as a phosphate exit after GTP has been hydrolyzed.

The identification of the putative binding site either for a coGAP or for the precursor protein is helped by two observations. We identified a hydrophobic cavity inside the structure of Toc33/34

Figure 1. Toc34 from Pisum sativum Is Dimeric

(A) The protein is shown as a ribbon diagram with GMPPNP in stick representation. The magnesium ion is colored in green; secondary structure elements are indicated. The monomer on the right-hand side is colored in gray. The conserved box (CB), characteristic for the Aig1/Toc34/Toc159-like paraseptin family, is colored in red; compare alignment between Toc and Aig GTPases. Insertions within psToc34 compared to the small GTPase Ras p21 (PDB code: 5P21) (Pai et al., 1990) are shown in light blue in the structure. psArg133 is shown in stick representation. Residues not resolved in electron density are indicated by a dashed line.

(B) The dimer interface region is shown for psToc34 in the GMPPNP- (dark) and GDP-bound states (light). The nucleotide binding site of each monomer is part of the dimerization interface, made up of several loops. Three loop regions are highlighted: the G2/switch I and G3/switch II regions, the loop carrying psArg133 of the CB, and the loop following a5. The G2/switch I loop is shifted between GDP- and GMPPNP-bound states, as it must accommodate the g-phosphate.

(C) Analytical ultracentrifugation performed using freshly prepared psToc34, or GDP- or GMPPNP-exchanged proteins (concentration 50 mM monomer protein). For the sedimentation velocity runs, the distributions of sedimentation coefficients are shown. The s values were corrected for solvent density and viscosity of the buffer (standard conditions $s_{20,w}$ for 20 C, H_2O).

(D) The apparent single-turnover rate constants for indicated concentrations of psToc34 were determined at pH 8 (see Experimental Procedures). Measurement in the concentration range from 0.013 to 4.5 mM protein covers the stoichiometric point of dimer formation.

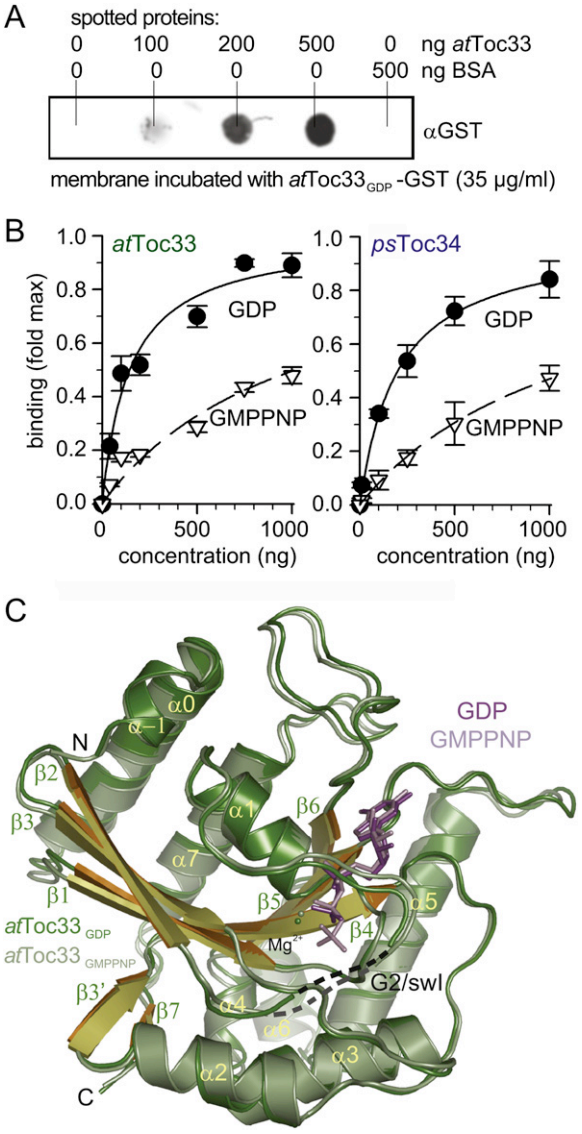

Figure 2. Monomeric atToc33

(A) Indicated amounts of His_6-tagged $atToc33_{GDP}$ or BSA (control) were immobilized on nitrocellulose; the membrane was subsequently incubated with $atToc33\text{-}GST_{GDP}$ (at a concentration of 35 mg/ml). Binding was visualized by immunodecoration with anti-GST antibodies.

(B) Indicated amounts of atToc33-His (left) or psToc34-His (right) loaded with GDP (circles) or GMPPNP (triangles) were immobilized as in (A). The membrane was incubated with atToc33-GST (left) or psToc34-GST (right) loaded with GDP (circles) or GMPPNP (triangles). The amount of bound protein was quantified and plotted against the amount of the immobilized receptor. The average of at least five independent experiments is shown. The lines represent the least square fit to Equation 1.

(C) Ribbon diagram of atToc33 in the GMPPNP- (green) and GDP-bound (light green) states. The molecule is a monomer in the crystal. Structural elements, nucleotide, and magnesium are indicated. A small segment in the G2/switch I region is not resolved in electron density in either of the two structures.

(Figure 6A). The cavity is lined with the Toc GTPase-specific N-terminal extension, forming helices a1 and a0 (Figure 1A). This cavity is sizable, with a volume of 62 $Å^3$ when probed with a solvent sphere of 1.4 Å (calculated with VOIDOO; Kleywegt and Jones, 1994). Previous Toc33/34 structures also contain the cavity, although it has not been described (Sun et al., 2002; Yeh et al., 2007). Cavities inside proteins are generally energetically unfavorable, and might destabilize the protein structure (Matthews, 1996), which could explain the aging effect observed with Toc33/34 (see above). In addition, between the cavity and the G2/G3 elements, we find in two psToc34 protomers a bound polyethylene glycol (PEG) molecule. It lies in a shallow pocket which is an extension of the cavity and is formed by residues conserved in Toc33/34. The PEG molecule is bound by the residues Asn57, Glu62, and Arg63 (Figure 6B). It is a frequent crystallographic observation that binding of solvent molecules alludes to substrate binding pockets in enzymes or to protein-protein interaction sites (Becker et al., 1998; Bourne et al., 2001; Dollins et al., 2005). The shallow PEG binding pocket in the vicinity of switch I might be part of a binding site which is involved in the stabilization of this switch region, and hence could be the binding site for a coGAP. The cavity as well as the bound PEG molecule might be functionally important features of the GTPase—as discussed below—that need to be further explored.

DISCUSSION

The two GTPases atToc33 and psToc34 are functional homologs (Jelic et al., 2003), and share a common 3D fold (Sun et al., 2002; Yeh et al., 2007). Extending from earlier studies, we demonstrate that the two GTPases have similar conformations in GDP- and GMPPNP-bound states (Figures 1 and 2). It is documented that both GTPases dimerize in a concentration-dependent manner: for atToc33, dimerization was shown using native PAGE analysis (Weibel et al., 2003) or gel-filtration techniques (Yeh et al., 2007); for psToc34, dimerization was shown using gel-filtration (Sun et al., 2002) or analytical ultracentrifugation (Reddick et al., 2007). We confirm and quantify dimerization using analytical ultracentrifugation and determine the dissociation constant K_D for the $psToc34_{GDP}$ dimer to be 50 ± 20 mM (Figure 1C). We show that atToc33 has a higher dissociation constant than psToc34, and this fits previous modeling data where less polar contacts were seen for atToc33 than for psToc34, whereas the buried interface areas were similar in both cases (Yeh et al., 2007). The K_D for the atToc33 dimer is outside the measurable range for analytical ultracentrifugation, and thus we confirm dimerization using a filter binding assay (Figure 2B).

The functional relevance of dimerization is controversial (Sun et al., 2002; Weibel et al., 2003). An important dimer contact is seen in both $psToc34_{GMPPNP}$ (Figure 1) and $psToc34_{GDP}$ (Sun et al., 2002) through the conserved arginine psArg133, which inserts into the active site of the dimerization partner. Consequently, mutation of this residue abrogates dimerization (Reddick et al., 2007; Weibel et al., 2003). Mutagenesis data are also somewhat controversial. When replacing the conserved arginine in atToc33 by alanine, either no (Weibel et al., 2003) or only a minor reduction in catalytic rate is observed (Yeh et al., 2007). The same replacement in psToc34, however, leads to a drastic decrease in hydrolysis rate (Reddick et al., 2007). The differences in dimerization behavior between the two proteins reported here could in part explain these contradictory results. An important issue is whether the arginine serves a role as an

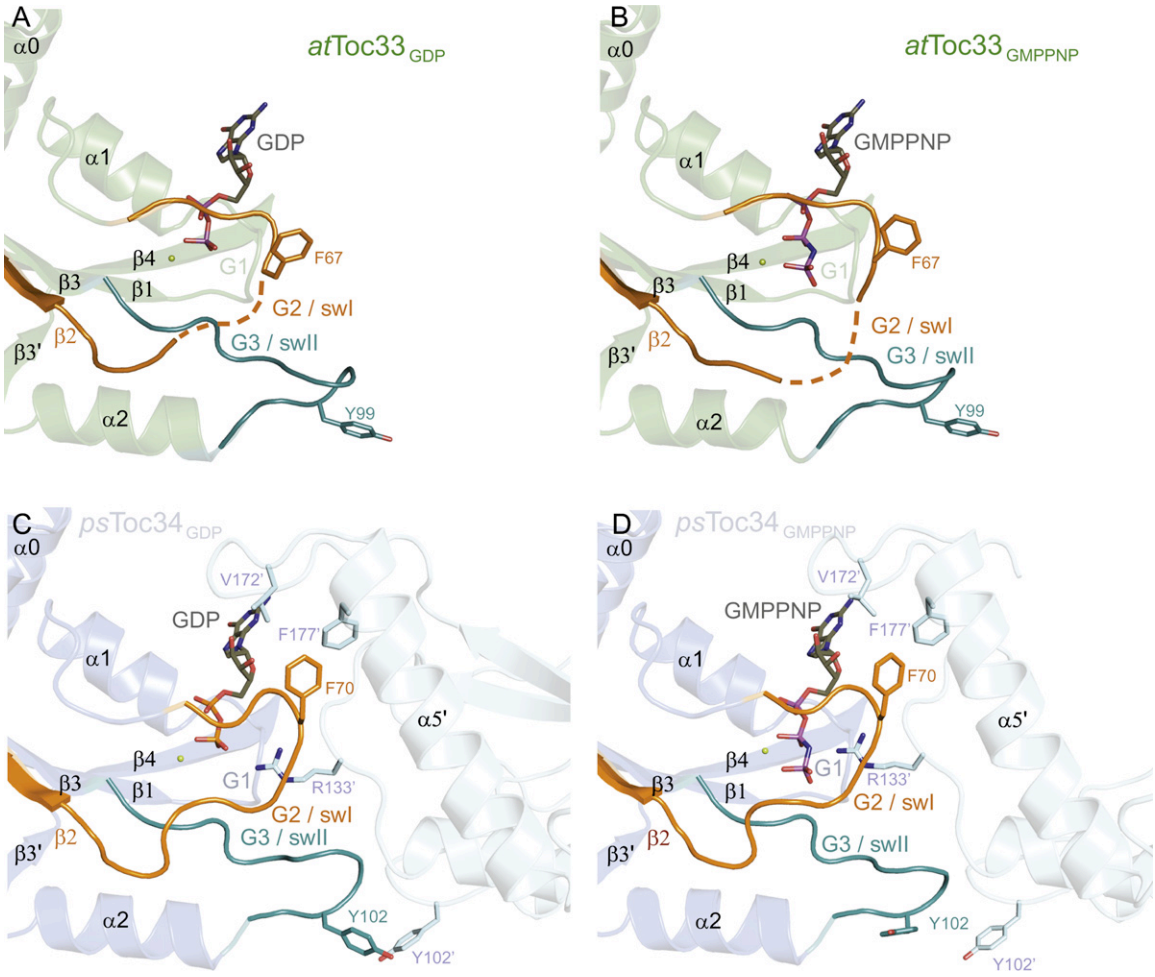

Figure 3. Comparison of the Switch Regions and the Dimerization Interface of atToc33 and psToc34

(A and B) G2/switch I and G3/switch II regions in monomeric $atToc33_{GDP}$ (A) and $atToc33_{GMPPNP}$ (B). Only selected secondary structure elements are shown for clarity; GMPPNP is shown in stick representation. Residues Ala69 and Glu70 are not resolved in electron density (dashed line).

(C and D) G2/switch I and G3/switch II regions in dimeric $psToc34_{GDP}$ (PDB code: 1H65) (Sun et al., 2002) (C) and $psToc34_{GMPPNP}$ (D). Only selected secondary structure elements are shown for clarity; GMPPNP is shown in stick representation. Arg133 of the CB from the second monomer is in contact with nucleotide. Phe70 of the G2/switch I region and Tyr102 of the G3/switch II region are seen in a dimer contact.

arginine finger (Sun et al., 2002), described before for GTPase-GAP complexes (Scheffzek et al., 1997, 1998) or reciprocally activated GTPase dimers such as the SRP GTPases FtsY and Ffh (Connolly and Gilmore, 1993; Egea et al., 2004; Focia et al., 2004), the GTPases hGBP belonging to the so-called large GTPases of the dynamin type (Prakash et al., 2000), or the GTPase MnmE involved in tRNA modification (Scrima and Wittinghofer, 2006). In all these cases, dimerization increases the intrinsic hydrolysis rate by one or two orders of magnitude, and dimerization preferentially occurs in the GTP-bound state, although a common mechanism or dimerization interface has not been derived. We demonstrate about 1.5-fold activation of psToc34 by dimerization, in keeping with previous reports on psToc34 (Reddick et al., 2007) and atToc33 (Yeh et al., 2007). Although this level of activation is far below the values reported for GTPase-GAP complexes (Scheffzek et al., 1998), the slight preference for dimerization in the GDP state also contradicts the GAP paradigm (Figures 1C and 2B). However, the latter result is susceptible to experimental error because of documented protein aging, and thus these data require further experimental clarification.

The biochemical data suggest the Toc33/34 homodimer is not a GAP complex, and this interpretation is supported by the structural data. The structures of $psToc34_{GMPPNP}$ in comparison with the one of $psToc34_{GDP}$ (Sun et al., 2002), or the structures of $atToc33_{GMPPNP}$ in comparison with $atToc33_{GDP}$, do not show any changes that would be consistent with GTPase activation (Figures 1 and 2). Indeed, that Toc33/34 would be optimized to function in the dimeric context, possibly forming important interactions with other proteins, is supported by two observations. First, the switch movement of psToc34 is reduced to the movement of psGlu73 and only seen in the dimeric state of the GTPase (Figure 5), that is, in psToc34. The GTPase cycle could then serve to modulate interaction with, for example, subunits of the Toc

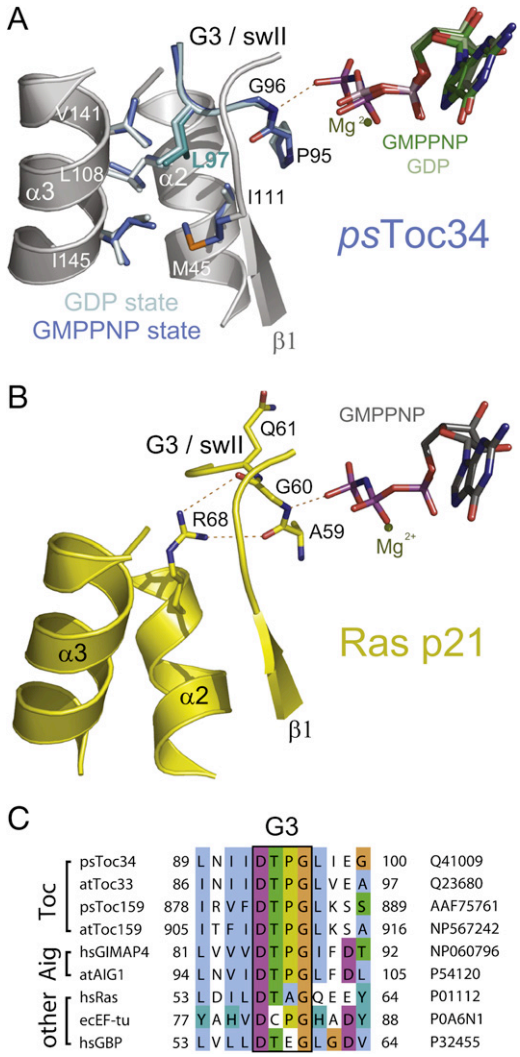

Figure 4. Comparison of the G3 Regions in psToc34 and Ras p21

(A) The conformation of G3/switch II is identical in the GMPPNP- and the GDP-bound states of psToc34. Gly96 is in hydrogen-bonding distance to the g-phosphate, and is conserved in the GTPase G3 motif (DxxG). Leu97, directly following the G3 motif, enters a hydrophobic pocket between helices a2 and a3.

(B) A similar representation as in (A) for G3/switch II of Ras p21 (PDB code: 5P21) (Pai et al., 1990). Gly60 is in hydrogen-bonding distance to the g-phosphate in the GMPPNP-bound state; different from psToc34, Gly60 is turned away from the binding pocket in the GDP-bound state of Ras p21 (not shown). The equivalent residue to Leu97 of psToc34 is the catalytic residue Gln61 in Ras p21, which is turned toward the nucleotide.

(C) The alignment shows the G3 region of six members of the Aig1/Toc34/Toc159-like paraseptin GTPase family, together with three GTPases of the TRAFAC class.

complex. The nucleotide load of psToc34 as sensed by psGlu73 would then regulate these interactions. Indeed, several reports have indicated that Toc34 interacts with other Toc components in a nucleotide-dependent manner, for example with the translocation pore Toc75 (Ertel et al., 2005) or the Toc subunit Toc64 (Qbadou et al., 2006). Second, like psGlu73, psArg133 can only perform its function in the GTPase dimer (Figure 3).

Although psArg133 is not able to activate GTP hydrolysis significantly (Figure 1D), examination of active site features in the psToc34 dimer shows that psArg133 might contribute to stabilizing a reaction intermediate of GTP hydrolysis (see Figure S5 for a comparison of psArg133 with typical arginine finger interactions). Intrinsic catalytic activity of psToc34 can be explained by the observation of a water molecule positioned for an attack on the g-phosphate (Figure 5). However, the positioning and probably the polarization of this water by the carbonyl oxygen of psGly74 are not ideal. In addition, this part of the G2/switch I element shows some flexibility (Figure S3), suggesting a coGAP is required to stabilize this element and to position the attacking water more properly. An alternative suggestion is that a coGAP directly supplies a catalytic residue to accelerate GTP hydrolysis. Interestingly, we find that the g-phosphate is accessible in the GMPPNP- but not in the GDP-bound state, through movement of the switch I glutamate psGlu73 (Figure 6D). The tunnel identified is ideally suited for a catalytic residue of an interacting coGAP to enter and position and polarize a water molecule. Other Toc subunits might act as coGAP, potentially recognizing psGlu73 in the GMPPNP-bound state of the GTPase. This would naturally fit the picture to ensure that the GTPase is in contact with the pore, to signal "ready".

Toc33/34 acts as a precursor protein receptor (Gutensohn et al., 2000; Jelic et al., 2003; Kouranov and Schnell, 1997; Schleiff et al., 2002). In fact, here we identify an internal cavity in Toc33/34 (Figure 6A; Figure S6) suitable for protein interaction. This cavity in Toc33/34 might be responsible for the observed aging effects of the recombinant proteins. We believe the features of this cavity to be of relevance and propose that binding of precursor protein could occur here. It will be interesting to probe for the conformational changes that are to be expected when the cavity engages in protein recognition. Interestingly, chloroplast transit peptides have a propensity to form amphipathic helices (Bruce, 2000), and thus an attractive hypothesis is exchange of helix a0 of Toc33/34 with the helical part of the signal peptide; the cavity would provide a void for accommodation of the side chains, as signal peptides vary in sequence. Importantly, helix a0 is a Toc33/34-specific feature, and contained neither in Toc159 nor in the Aig GTPases. Further, identification of a PEG molecule bound between the cavity and the switch I region in a shallow pocket on psToc34$_{GMPPNP}$ might extend the precursor protein binding site (Figure 6; Figure S6).

Besides homodimerization, heterodimerization of Toc33/34 with the GTP binding domain of Toc159 has been reported (Becker et al., 2004; Hiltbrunner et al., 2001; Smith et al., 2002; Wallas et al., 2003). The Toc33/34/Toc159 interaction is functionally divergent from the Toc33/34 homodimer, because psArg133, the arginine of the dimerization motif, is not conserved in register in Toc159 (Figure 1A, alignment), and because Toc159 also misses the switch I glutamate that senses nucleotide load. Instead, Toc159 contains the conserved threonine of consensus GTPases of the TRAFAC class (Leipe et al., 2002), and it might thus exhibit a different mechanism for GTP hydrolysis, even when in heterodimeric contact with the small GTPase. Comparing the sequences of the two G domains, we have noted a five amino acid insertion in the Toc159 sequences inside the dimerization motif, in the loop connecting b5 with a5. When this insertion is modeled onto the dimeric psToc34 structure (Figure 6B, yellow), it is close to the

All rights reserved

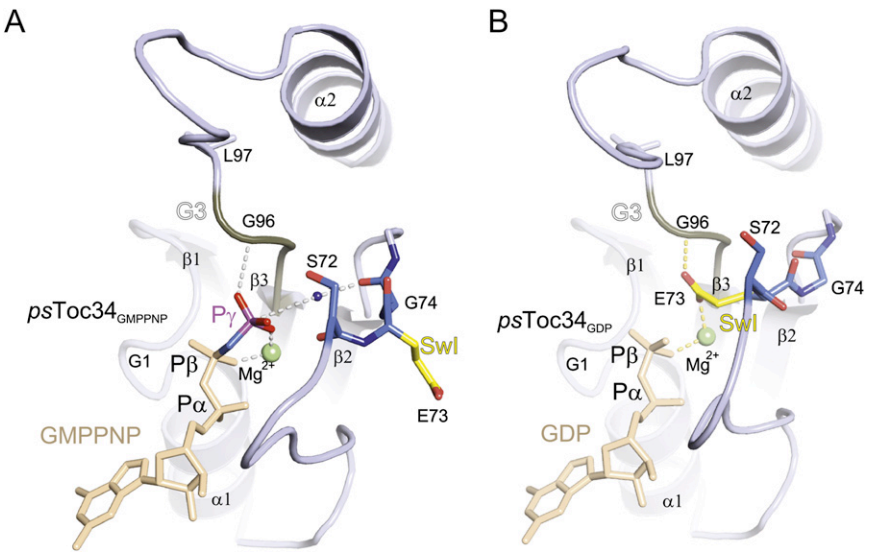

Figure 5. Glu73 of G2/Switch I Senses the Nucleotide Loading State in Dimeric psToc34

(A) psGlu73 is solvent exposed in psToc34 in the GMPPNP-bound state. A water that might be in position for nucleophilic attack on the g-phosphate is shown as a small blue sphere. The water is in hydrogen-bonding distance to Gly74 of the G2 region.

(B) In the GDP-bound state (PDB code: 1H65) (Sun et al., 2002), psGlu73 is turned toward the nucleotide and takes the position of the g-phosphate. It then coordinates the Mg^{2+} ion.

G2 element of psToc34 and thus in a very suggestive position for stabilization of this loop. The potential binding site for the Toc159 insertion is highly conserved among Toc33/34 GTPases, as can be shown by conservation mapping (Figure S6A). Further, the insertion partly overlaps with the bound PEG molecule that was fortuitously observed in our $psToc34_{GMPPNP}$ structure (Figure 6; Figure S6). Thus, binding of precursor protein and formation of the heterodimer might be linked, as previously suggested (Becker et al., 2004). Toc159 additionally contains two auxiliary domains which might be involved in the regulation of heterodimer formation. In contrast to the symmetric Toc33/34 homodimer, the asymmetric Toc33/34/Toc159 heterodimer could thus be self-regulating.

It is thus plausible that two distinct and different dimerization events take place during a translocation cycle. First, homodimerization of Toc33/34 might occur as presented in this study. Observed stoichiometries within the Toc complex are consistent with homodimerization of the Toc33/34 subunits (Kikuchi et al., 2006; Schleiff et al., 2003). However, GTPase activity in the Toc33/34 homodimer probably requires regulation by external factors. Second, a self-regulated Toc33/34/Toc159 heterodimer might form. The disintegration of one dimer is a prerequisite for the formation of the second dimer. We are currently investigating in which order these dimerization events occur, and trying to establish the context in which one interaction is replaced by the other. Identification of the proposed coGAP and mapping of precursor protein interaction are further of the essence to promote insights into the GTPase cycle of Toc33/34. This analysis is challenging because the Toc proteins are membrane associated, and regulators such as coGAPs might be integral to the membrane.

EXPERIMENTAL PROCEDURES

Protein Expression, Purification, and Nucleotide Exchange

cDNA encoding $psToc34_{1–266}$ was ligated with pET21d between the Nco1 and Xho1 restriction sites. $atToc33_{S181E\ 1–251}$ and $psToc34_{E10G\ 1–266}$ were generated by PCR using $atToc33_{1–251}$ (Jelic et al., 2003) or $psToc34_{1–266}$ as template and were cloned into pET21d (Novagen, Madison, WI, USA) to generate $atToc33_{1–251}$-His, $atToc33_{S181E\ 1–251}$-His, $psToc34_{1–266}$, and $psToc34_{E10G\ 1–266}$ or into pGEX-6P-1 to generate $atToc33_{1–251}$-GST (GE Healthcare, Freiburg, Germany). Unless otherwise noted, psToc34 and atToc33 denote His-tagged proteins that were purified using Ni-NTA affinity chromatography (Jelic et al., 2003). For crystallization and single-turnover hydrolysis assays, the proteins were additionally purified by gel-filtration chromatography using a Superdex 75 HR 26/60 column (GE Healthcare) with 20 mM HEPES (pH 7.4) containing 150 mM KCl, 3 mM $MgCl_2$, and 0.7 mM b-mercaptoethanol as running buffer. GST-tagged proteins were purified according to the manufacturer's instructions (GE Healthcare).

For nucleotide exchange, the proteins at a concentration of 1 mM were incubated overnight at 4 C with 2 mM GMPPNP (all nucleotides and analogs from Sigma-Aldrich, Schnelldorf, Germany) and with 50 U alkaline phosphatase (New England Biolabs, Frankfurt am Main, Germany). Unbound nucleotides were removed by buffer exchange using a PD-10 column (GE Healthcare). The individual loading state was controlled by RP-HPLC analysis using a C_{18} column (Vydac, Hesperia, CA, USA) on a Merck HPLC system equipped with an L4500 detector (running buffer: 100 mM phosphate buffer [pH 6.5], 10 mM tetrabutylammonium bromide, 7.5% acetonitrile) (Tucker et al., 1986).

Crystallization and Structure Determination

Purified proteins were concentrated to 0.5 mM and crystallized at 19 C, using the sitting-drop vapor-diffusion technique with a 2 ml drop size. Crystals of $psToc34_{GMPPNP}$ were typically obtained within 1 d in 0.2 M dipotassium phosphate and 20% PEG3350. Crystals of $atToc33_{GMPPNP}$ were typically obtained within 3 d in 22% PEG1500 and 15% glycerol. Crystals of $atToc33_{GDP}$ were obtained within 3 d in 24% PEG1500 and 20% (v/v) glycerol. Crystals were harvested in cryoprotectant buffer containing 25% glycerol and flash-frozen for storage in liquid nitrogen. Point mutations introduced into $atToc33_{GMPPNP}$ and $psToc34_{GMPPNP}$ improved crystal quality and were used for the structural analyses: atToc33 was crystallized as S181E variant; psToc34 was crystallized as E10G variant. The amino acid exchanges have no influence on tertiary structure, as seen here.

Data were collected on the tunable beamline ID23-1 at the European Synchrotron Radiation Facility, Grenoble, France. Data were integrated and scaled with HKL software (Otwinowski and Minor, 1997). Data reduction, free R assignment, and all further data manipulation were carried out with the CCP4 suite of programs (CCP4, 1994). The structures were determined by molecular replacement using the program MOLREP (Vagin and Teplyakov, 1997) with psToc34 GDP (Sun et al., 2002) as a search model for psToc34 GMPPNP. Iterative model building and refinement were carried out with the programs Coot (Emsley and Cowtan, 2004) and REFMAC5 (Murshudov et al., 1997), cycled with ARP (Lamzin and Wilson, 1997). Structure quality was accessed using PROCHECK (Laskowski et al., 1993), and data have been deposited in the PDB under codes 3BB1, 3BB3, and 3BB4.

Analytical Ultracentrifugation, Solid-Phase Binding, and GTP Single Turnover

For analytical ultracentrifugation, psToc34 was loaded on a nickel affinity column in 20 mM Tris (pH 8.5) containing 100 mM NaCl, 1 mM $MgCl_2$, 10 mM arginine, 10 mM imidazole, and 5% glycerol and eluted using an equivalent

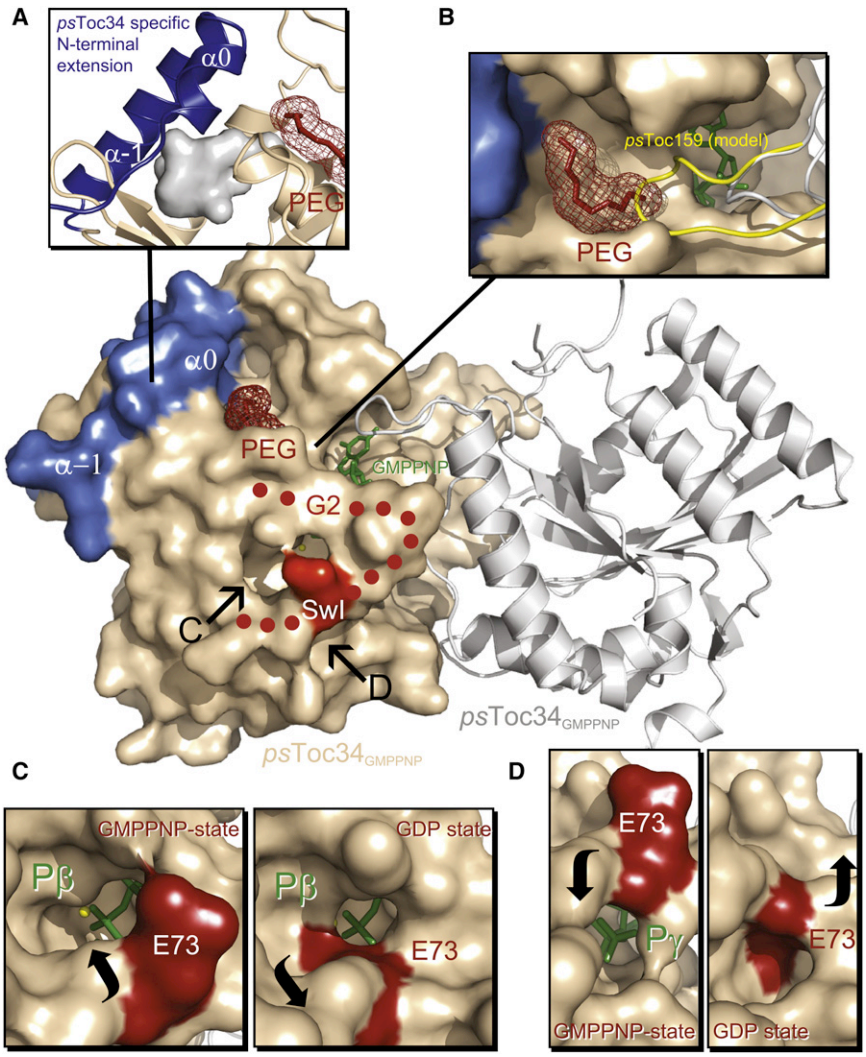

Figure 6. Potential Binding Sites on the Surface of psToc34

The psToc34$_{GMPPNP}$ dimer, with one monomer shown in surface representation and another monomer shown in cartoon representation. The Toc34-specific N-terminal extensions and G2/switch I are shown in blue and red, respectively. Bound GMPPNP is colored in green, and a bound PEG molecule, arising from the crystallization buffer, is colored in dark red.

(A) A cavity of 63 Å^3 (gray) is identified between helix a1, helix a0, and the central b sheet of the GTPase domain.

(B) The PEG molecule binds in a shallow pocket on the surface of psToc34, between the cavity and close to the G2 element. In dimeric psToc34, this shallow pocket forms a binding site for the loop following helix a5, gray. In psToc159, a sequence insertion of four residues is identified in this loop; the loop has been modeled into the dimer, shown in yellow.

(C and D) The b- and g-phosphates of GMPPNP nucleotide are accessible through tunnels from the surface in dimeric psToc34.

(C) The tunnel toward b-phosphate is open in the GMPPNP- and the GDP-bound states of psToc34. However, the tunnel is enlarged by the movement of the switch residue Glu73 in psToc34$_{GMPPNP}$.

(D) The tunnel toward the g-phosphate is closed in psToc34$_{GDP}$ but opened in psToc34$_{GMPPNP}$, through movement of the switch residue Glu73.

buffer containing 250 mM imidazole. Afterward, the buffer was exchanged with 20 mM Tris (pH 8.5) containing 100 mM NaCl, 5 mM EDTA, 10 mM arginine, 10 mM imidazole, and 5% glycerol using a PD-10 column. GMPPNP nucleotide exchange was performed as described; GDP nucleotide exchange was performed using protein at a concentration of 1 mM incubated with 10 mM GDP overnight at 4 C. Subsequently, the proteins were gel filtered using a Superdex 75 26/60 size-exclusion column using the nickel affinity purification buffer. The nucleotide loading states of the proteins were controlled by HPLC analysis.

For sedimentation velocity studies, a Beckman Optima XL-A ultracentrifuge equipped with absorbance optics and an An60 Ti rotor (Beckman Coulter, Fullerton, CA, USA) was used. Centrifugation runs were carried out at 20 C at 40,000 rpm using a concentration of 50 mM monomer protein and purification buffer as reference. Buffer density (1.01759 ml/g), buffer viscosity (1.1832 mPa s), as well as the partial specific volume of psToc34 based on the amino acid sequence ($\bar{\nu}$ = 0.7410 ml/g) were calculated using the program SEDNTERP, version 1.05 (J. Philo, D. Hayes, and T. Laue, http://www.jphilo.mailway.com/download.htm/). The apparent sedimentation coefficient and molecular weight distributions c(s) and c(M) were determined with the program SEDFIT (Dam and Schuck, 2004; Schuck, 2000). Dissociation constants were derived from fitting the sedimentation velocity data with SEDPHAT to a monomer-dimer equilibrium model (Schuck, 2003).

For determination of nucleotide-dependent association, atToc33 was preloaded with nucleotides and spotted onto nitrocellulose membranes using a 96-well vacuum manifold (Bethesda Research Laboratories, Bethesda, MD, USA). Nitrocellulose membranes were saturated with 0.3% low-fat milk powder with 0.03% BSA and then incubated with purified GST-atToc33 (35 mg/ml) preloaded with the indicated nucleotides in 20 mM tricine-KOH (pH 7.6) containing 100 mM NaCl and 1 mM $MgCl_2$. Background binding was controlled by incubation of GST-atToc33 with empty or BSA-coated nitrocellulose membranes. After two washes (10 min), the bound protein was determined by immunodecoration with GST antibodies. Intensities were quantified with AIDA software (Raytest, Straubenhardt, Germany). The amount of bound protein was corrected for background staining of the blot and expressed in comparison to the maximal binding of wild-type protein. The binding was analyzed by

$$\%\text{Bound}_{\text{norm:}} = \left[\frac{1}{4}\left(S + E + K\right)^2 - S \cdot E + \frac{1}{2}\left(S + E + K\right)\right] \quad (1)$$

where S is the concentration of the spotted protein, E is the concentration of the added protein (normalized), and K reflects the dissociation constant in a nonnormalized situation and an apparent dissociation constant after normalization. A detailed derivation of Equation 1 is presented in Supplemental Data.

For GTP nucleotide single-turnover hydrolysis, psToc34 was exchanged with 20 mM HEPES (pH 7.4) containing 75 mM KCl and 5 mM EDTA using a PD-10 column before incubation overnight at 4 C with 30 mM GTP. Excess nucleotide was removed using a PD-10 desalting column (GE Healthcare), and equilibrated with 20 mM Tris-HCl (pH 8.0) containing 75 mM KCl and 5 mM $MgCl_2$. GTP single-turnover hydrolysis (Prakash et al., 2000) was carried out at 20 C. GTP:GDP ratios of aliquots from the reaction mixture taken at different time points were determined by RP-HPLC analysis. From the changes in the GTP:GDP ratio over time, starting with GTP-loaded proteins, the area of the nucleotide peaks was determined by a Weibull function and the GDP fraction was calculated. The apparent hydrolysis rate was determined by an exponential function and the distribution of the apparent rate constants was analyzed by

$$k_{app} = D=T \quad k_D + \eth T \quad D\text{Þ}=T \quad k_M; \qquad (2)$$

with k_{app} the apparent rate constant, D the concentration of the receptor in the dimeric state, T the total receptor concentration, and k_D or K_M the rate constant for the dimeric and monomeric receptor, respectively. For details on how Equation 2 is derived, see Supplemental Data.

ACCESSION NUMBERS

Coordinates and structure factors for $psToc34_{GMPPNP}$, $atToc33_{GDP}$, and $atToc33_{GMPPNP}$ have been deposited in the Protein Data Bank under ID codes 3BB1, 3BB3, and 3BB4, respectively.

SUPPLEMENTAL DATA

Supplemental Data include seven figures and Supplemental Experimental Procedures and can be found with this article online at http://www.structure.org/cgi/content/full/16/4/585/DC1/.

ACKNOWLEDGMENTS

We thank Nico Eisele, Felix Findeisen, Johannes Melchers, and Maike Ruprecht for experimental support, staff at the ESRF synchrotron for help with data collection, and Gert Bange, Klemens Wild, and Klaus Scheffzek for critical discussion. The work was supported by grants from the Deutsche Forschungsgemeinschaft (SFB594-B11) and the Cluster of Excellence Frankfurt Macromolecular Complexes (CEF) to E.S., by the Volkswagenstiftung to E.S. and K.R., and by the interdisciplinary PhD program "Molecular Machines: Mechanisms and Functional Interconnections" of the Land Baden-Württemberg to I.S.

Received: September 17, 2007
Revised: January 18, 2008
Accepted: January 22, 2008
Published: April 8, 2008

REFERENCES

Bauer, J., Hiltbrunner, A., Weibel, P., Vidi, P.A., Alvarez-Huerta, M., Smith, M.D., Schnell, D.J., and Kessler, F. (2002). Essential role of the G-domain in targeting of the protein import receptor atToc159 to the chloroplast outer membrane. J. Cell Biol. 159, 845–854.

Becker, A., Schlichting, I., Kabsch, W., Groche, D., Schultz, S., and Wagner, A.F. (1998). Iron center, substrate recognition and mechanism of peptide deformylase. Nat. Struct. Biol. 5, 1053–1058.

Becker, T., Jelic, M., Vojta, A., Radunz, A., Soll, J., and Schleiff, E. (2004). Preprotein recognition by the Toc complex. EMBO J. 23, 520–530.

Bourne, H.R., Sanders, D.A., and McCormick, F. (1991). The GTPase superfamily: conserved structure and molecular mechanism. Nature 349, 117–127.

Bourne, Y., Dannenberg, J., Pollmann, V., Marchot, P., and Pongs, O. (2001). Immunocytochemical localization and crystal structure of human frequenin (neuronal calcium sensor 1). J. Biol. Chem. 276, 11949–11955.

Bruce, B.D. (2000). Chloroplast transit peptides: structure, function and evolution. Trends Cell Biol. 10, 440–447.

CCP4 (Collaborative Computational Project, Number 4) (1994). The CCP4 suite: programs for protein crystallography. Acta Crystallogr. D Biol. Crystallogr. 50, 760–763.

Chen, K., Chen, X., and Schnell, D.J. (2000). Initial binding of preproteins involving the Toc159 receptor can be bypassed during protein import into chloroplasts. Plant Physiol. 122, 813–822.

Connolly, T., and Gilmore, R. (1993). GTP hydrolysis by complexes of the signal recognition particle and the signal recognition particle receptor. J. Cell Biol. 123, 799–807.

Constan, D., Patel, R., Keegstra, K., and Jarvis, P. (2004). An outer envelope membrane component of the plastid protein import apparatus plays an essential role in Arabidopsis. Plant J. 38, 93–106.

Dam, J., and Schuck, P. (2004). Calculating sedimentation coefficient distributions by direct modeling of sedimentation velocity concentration profiles. Methods Enzymol. 384, 185–212.

Dollins, D.E., Immormino, R.M., and Gewirth, D.T. (2005). Structure of unliganded GRP94, the endoplasmic reticulum Hsp90. Basis for nucleotide-induced conformational change. J. Biol. Chem. 280, 30438–30447.

Egea, P.F., Shan, S.O., Napetschnig, J., Savage, D.F., Walter, P., and Stroud, R.M. (2004). Substrate twinning activates the signal recognition particle and its receptor. Nature 427, 215–221.

Emsley, P., and Cowtan, K. (2004). Coot: model-building tools for molecular graphics. Acta Crystallogr. D Biol. Crystallogr. 60, 2126–2132.

Ertel, F., Mirus, O., Bredemeier, R., Moslavac, S., Becker, T., and Schleiff, E. (2005). The evolutionarily related b-barrel polypeptide transporters from Pisum sativum and Nostoc PCC7120 contain two distinct functional domains. J. Biol. Chem. 280, 28281–28289.

Focia, P.J., Shepotinovskaya, I.V., Seidler, J.A., and Freymann, D.M. (2004). Heterodimeric GTPase core of the SRP targeting complex. Science 303, 373–377.

Garcia de la Torre, J., Navarro, S., Lopez Martinez, M.C., Diaz, F.G., and Lopez Cascales, J.J. (1994). HYDRO: a computer program for the prediction of hydrodynamic properties of macromolecules. Biophys. J. 67, 530–531.

Goldberg, J. (1999). Structural and functional analysis of the ARF1-ARFGAP complex reveals a role for coatomer in GTP hydrolysis. Cell 96, 893–902.

Gutensohn, M., Schulz, B., Nicolay, P., and Flugge, U.I. (2000). Functional analysis of the two Arabidopsis homologues of Toc34, a component of the chloroplast protein import apparatus. Plant J. 23, 771–783.

Hiltbrunner, A., Bauer, J., Vidi, P.A., Infanger, S., Weibel, P., Hohwy, M., and Kessler, F. (2001). Targeting of an abundant cytosolic form of the protein import receptor at Toc159 to the outer chloroplast membrane. J. Cell Biol. 154, 309–316.

Ivanova, Y., Smith, M.D., Chen, K., and Schnell, D.J. (2004). Members of the Toc159 import receptor family represent distinct pathways for protein targeting to plastids. Mol. Biol. Cell 15, 3379–3392.

Jelic, M., Sveshnikova, N., Motzkus, M., Horth, P., Soll, J., and Schleiff, E. (2002). The chloroplast import receptor Toc34 functions as preprotein-regulated GTPase. Biol. Chem. 383, 1875–1883.

Jelic, M., Soll, J., and Schleiff, E. (2003). Two Toc34 homologues with different properties. Biochemistry 42, 5906–5916.

Kessler, F., and Schnell, D.J. (2004). Chloroplast protein import: solve the GTPase riddle for entry. Trends Cell Biol. 14, 334–338.

Kessler, F., and Schnell, D.J. (2006). The function and diversity of plastid protein import pathways: a multilane GTPase highway into plastids. Traffic 7, 248–257.

Kikuchi, S., Hirohashi, T., and Nakai, M. (2006). Characterization of the preprotein translocon at the outer envelope membrane of chloroplasts by blue native PAGE. Plant Cell Physiol. 47, 363–371.

Kleffmann, T., Hirsch-Hoffmann, M., Gruissem, W., and Baginsky, S. (2006). plprot: a comprehensive proteome database for different plastid types. Plant Cell Physiol. 47, 432–436.

Kleywegt, G.J., and Jones, T.A. (1994). Detection, delineation, measurement and display of cavities in macromolecular structures. Acta Crystallogr. D Biol. Crystallogr. 50, 178–185.

Kouranov, A., and Schnell, D.J. (1997). Analysis of the interactions of preproteins with the import machinery over the course of protein import into chloroplasts. J. Cell Biol. 139, 1677–1685.

Krucken, J., Schroetel, R.M., Muller, I.U., Saidani, N., Marinovski, P., Benten, W.P., Stamm, O., and Wunderlich, F. (2004). Comparative analysis of the human gimap gene cluster encoding a novel GTPase family. Gene 341, 291–304.

Krucken, J., Epe, M., Benten, W.P., Falkenroth, N., and Wunderlich, F. (2005). Malaria-suppressible expression of the anti-apoptotic triple GTPase mGIMAP8. J. Cell. Biochem. 96, 339–348.

Lamzin, V.S., and Wilson, K.S. (1997). Automated refinement for protein crystallography. Methods Enzymol. 277, 269–305.

Laskowski, R.A., MacArthur, M.W., Moss, D.S., and Thornton, J.M. (1993). PROCHECK: a program to check the stereochemical quality of protein structures. J. Appl. Crystallogr. 26, 283–291.

Leipe, D.D., Wolf, Y.I., Koonin, E.V., and Aravind, L. (2002). Classification and evolution of P-loop GTPases and related ATPases. J. Mol. Biol. 317, 41–72.

Leister, D. (2003). Chloroplast research in the genomic age. Trends Genet. 19, 47–56.

Li, H.M., Kesavulu, M.M., Su, P.H., Yeh, Y.H., and Hsiao, C.D. (2007). Toc GTPases. J. Biomed. Sci. 14, 505–508.

Matthews, B.W. (1996). Structural and genetic analysis of the folding and function of T4 lysozyme. FASEB J. 10, 35–41.

Mishra, R., Gara, S.K., Mishra, S., and Prakash, B. (2005). Analysis of GTPases carrying hydrophobic amino acid substitutions in lieu of the catalytic glutamine: implications for GTP hydrolysis. Proteins 59, 332–338.

Murshudov, G.N., Vagin, A.A., and Dodson, E.J. (1997). Refinement of macromolecular structures by the maximum-likelihood method. Acta Crystallogr. D Biol. Crystallogr. 53, 240–255.

Nitta, T., and Takahama, Y. (2007). The lymphocyte guard-IANs: regulation of lymphocyte survival by IAN/GIMAP family proteins. Trends Immunol. 28, 58–65.

Oreb, M., Reger, K., and Schleiff, E. (2006). Chloroplast protein import: reverse genetic approaches. Curr. Genomics 7, 235–244.

Otwinowski, Z., and Minor, W. (1997). Processing of X-ray diffraction data collected in oscillation mode. Methods Enzymol. 276, 307–326.

Pai, E.F., Krengel, U., Petsko, G.A., Goody, R.S., Kabsch, W., and Wittinghofer, A. (1990). Refined crystal structure of the triphosphate conformation of H-ras p21 at 1.35 Å resolution: implications for the mechanism of GTP hydrolysis. EMBO J. 9, 2351–2359.

Prakash, B., Praefcke, G.J., Renault, L., Wittinghofer, A., and Herrmann, C. (2000). Structure of human guanylate-binding protein 1 representing a unique class of GTP-binding proteins. Nature 403, 567–571.

Qbadou, S., Becker, T., Mirus, O., Tews, I., Soll, J., and Schleiff, E. (2006). The molecular chaperone Hsp90 delivers precursor proteins to the chloroplast import receptor Toc64. EMBO J. 25, 1836–1847.

Reddick, L.E., Vaughn, M.D., Wright, S.J., Campbell, I.M., and Bruce, B.D. (2007). In vitro comparative kinetic analysis of the chloroplast Toc GTPases. J. Biol. Chem. 282, 11410–11426.

Reuber, T.L., and Ausubel, F.M. (1996). Isolation of Arabidopsis genes that differentiate between resistance responses mediated by the RPS2 and RPM1 disease resistance genes. Plant Cell 8, 241–249.

Scheffzek, K., and Ahmadian, M.R. (2005). GTPase activating proteins: structural and functional insights 18 years after discovery. Cell. Mol. Life Sci. 62, 3014–3038.

Scheffzek, K., Ahmadian, M.R., Kabsch, W., Wiesmuller, L., Lautwein, A., Schmitz, F., and Wittinghofer, A. (1997). The Ras-RasGAP complex: structural basis for GTPase activation and its loss in oncogenic Ras mutants. Science 277, 333–338.

Scheffzek, K., Ahmadian, M.R., and Wittinghofer, A. (1998). GTPase-activating proteins: helping hands to complement an active site. Trends Biochem. Sci. 23, 257–262.

Schleiff, E., Soll, J., Sveshnikova, N., Tien, R., Wright, S., Dabney-Smith, C., Subramanian, C., and Bruce, B.D. (2002). Structural and guanosine triphosphate/diphosphate requirements for transit peptide recognition by the cytosolic domain of the chloroplast outer envelope receptor, Toc34. Biochemistry 41, 1934–1946.

Schleiff, E., Soll, J., Kuchler, M., Kuhlbrandt, W., and Harrer, R. (2003). Characterization of the translocon of the outer envelope of chloroplasts. J. Cell Biol. 160, 541–551.

Schuck, P. (2000). Size-distribution analysis of macromolecules by sedimentation velocity ultracentrifugation and Lamm equation modeling. Biophys. J. 78, 1606–1619.

Schuck, P. (2003). On the analysis of protein self-association by sedimentation velocity analytical ultracentrifugation. Anal. Biochem. 320, 104–124.

Schweins, T., Geyer, M., Scheffzek, K., Warshel, A., Kalbitzer, H.R., and Wittinghofer, A. (1995). Substrate-assisted catalysis as a mechanism for GTP hydrolysis of p21ras and other GTP-binding proteins. Nat. Struct. Biol. 2, 36–44.

Scrima, A., and Wittinghofer, A. (2006). Dimerisation-dependent GTPase reaction of MnmE: how potassium acts as GTPase-activating element. EMBO J. 25, 2940–2951.

Seewald, M.J., Kraemer, A., Farkasovsky, M., Korner, C., Wittinghofer, A., and Vetter, I.R. (2003). Biochemical characterization of the Ran-RanBP1-RanGAP system: are RanBP proteins and the acidic tail of RanGAP required for the Ran-RanGAP GTPase reaction? Mol. Cell. Biol. 23, 8124–8136.

Smith, M.D., Hiltbrunner, A., Kessler, F., and Schnell, D.J. (2002). The targeting of the atToc159 preprotein receptor to the chloroplast outer membrane is mediated by its GTPase domain and is regulated by GTP. J. Cell Biol. 159, 833–843.

Sprang, S.R. (1997). G protein mechanisms: insights from structural analysis. Annu. Rev. Biochem. 66, 639–678.

Sun, Y.J., Forouhar, F., Li, H.-m., Tu, S.L., Yeh, Y.H., Kao, S., Shr, H.L., Chou, C.C., Chen, C., and Hsiao, C.D. (2002). Crystal structure of pea Toc34, a novel GTPase of the chloroplast protein translocon. Nat. Struct. Biol. 9, 95–100.

Tucker, J., Sczakiel, G., Feuerstein, J., John, J., Goody, R.S., and Wittinghofer, A. (1986). Expression of p21 proteins in Escherichia coli and stereochemistry of the nucleotide-binding site. EMBO J. 5, 1351–1358.

Vagin, A.A., and Teplyakov, A. (1997). MOLREP: an automated program for molecular replacement. J. Appl. Crystallogr. 30, 1022–1025.

Vetter, I.R., and Wittinghofer, A. (2001). The guanine nucleotide-binding switch in three dimensions. Science 294, 1299–1304.

Vojta, A., Alavi, M., Becker, T., Hormann, F., Kuchler, M., Soll, J., Thomson, R., and Schleiff, E. (2004). The protein translocon of the plastid envelopes. J. Biol. Chem. 279, 21401–21405.

Wallas, T.R., Smith, M.D., Sanchez-Nieto, S., and Schnell, D.J. (2003). The roles of Toc34 and Toc75 in targeting the Toc159 preprotein receptor to chloroplasts. J. Biol. Chem. 278, 44289–44297.

Weibel, P., Hiltbrunner, A., Brand, L., and Kessler, F. (2003). Dimerization of Toc-GTPases at the chloroplast protein import machinery. J. Biol. Chem. 278, 37321–37329.

Yeh, Y.H., Kesavulu, M.M., Li, H.M., Wu, S.Z., Sun, Y.J., Konozy, E.H., and Hsiao, C.D. (2007). Dimerization is important for the GTPase activity of chloroplast translocon components atToc33 and psToc159. J. Biol. Chem. 282, 13845–13853.

Structure *16*

Supplemental Data

The GTPase Cycle of the Chloroplast Import Receptors Toc33/Toc34: Implications from Monomeric and Dimeric Structures

Patrick Koenig, Mislav Oreb, Anja Höfle, Sabine Kaltofen, Karsten Rippe, Irmgard Sinning, Enrico Schleiff, and Ivo Tews

Supplemental Experimental Procedures

Calculation of the Solid Phase Binding

Equation

$$[Bound] = -\,\mathrm{sqrt}[\,(K+S+E)^2 / 4 - S*E] + (K+S+E)/2 \qquad \text{(E1)}$$

is derived from

$$K = [E]*[S]/[Bound] \qquad \text{(E3)}$$

where $[S]$ is the free concentration of spotted protein, $[E]$ the free concentration of added protein (normalized), $[Bound]$ is the concentration of complexes formed and K the dissociation constant in a not normalized situation and an apparent dissociation constant after normalization. Considering the two relations

$$[E] = E - [Bound] \qquad \text{(E4)}$$

and

$$[S] = S - [Bound] \qquad \text{(E5)}$$

where S is the total concentration of spotted protein, and E the total concentration of added protein (normalized), equation (E3) can be written as

$$K = (E - [Bound])*(\,S - [Bound])/[Bound] \qquad \text{(E1')}$$

which can be rewritten as

$$[Bound] = \pm\,\mathrm{sqrt}[\,(K+S+E)^2 / 4 - S*E] + (K+S+E)/2 \qquad \text{(E6)}$$

The decision for the negative algebraic sign in equation (E1) comes from the following simple consideration: suppose *S* is zero, then [*Bound*] must be zero as well, which satisfied with negative algebraic sign.

Calculation of the Hydrolysis Rate

The apparent rate constants determined for different concentrations of the receptor can be analysed by equation (E2) for the following reason. The hydrolysis kinetic can be analyzed by

$$FH(t,T) = D/T * (1-\exp(-k_D*t)) + (T-D)/T * (1-\exp(-k_M*t)) \quad \text{(E7)}$$

with FH fold hydrolysis, D the concentration in dimeric conformation, T the total concentration of the GTPase, k_D the rate constant of the protein in dimeric conformation and the k_M rate constant in monomeric conformation. The apparent rate constant was determined at a given concentration by

$$FH(t)= 1-\exp(-k_{app}*t) \quad \text{(E8)}$$

can be written as

$$1-\exp(-k_{app}*t) = D/T*(1-\exp(-k_D*t))+(T-D)/T*(1-\exp(-k_M*t)) \quad \text{(E9)}$$

Hence, the following three transformations lead to the relation of the apparent rate constant

$$\exp(-k_{app}*t) = 1 - (D/T*(1-\exp(-k_D*t))+(T-D)/T*(1-\exp(-k_M*t))) \; k_{app}$$

$$= - \ln(1 - (D/T*(1-\exp(-k_D*t))+(T-D)/T*(1-\exp(-k_M*t))) / t \quad \text{(E10)}$$

Using the two approximations that $\ln(1-x) \sim - x$ and $\exp(x) \sim 1+x$ (both true since $x<1$), equation (E10) can be written as

$$k_{app}= D/T * k_D + (T-D)/T * k_M \quad \text{(E2)}$$

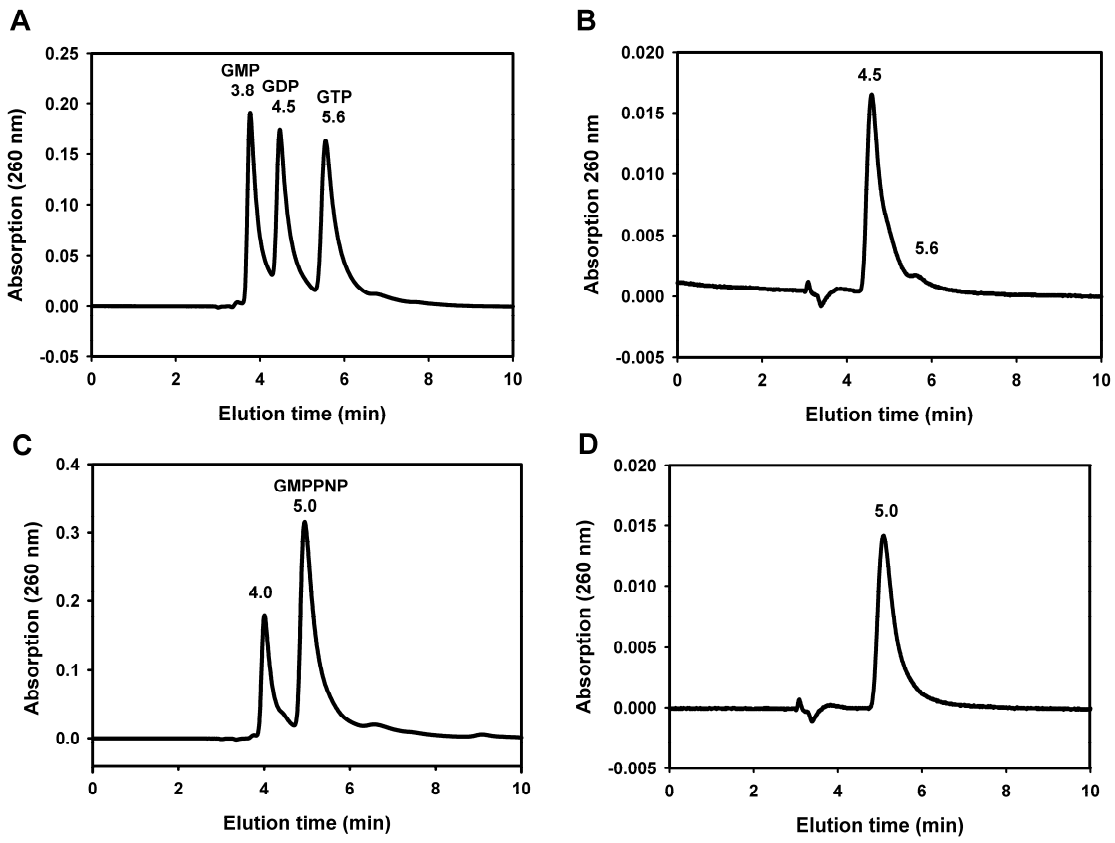

Figure S1. Nucleotide Binding State of *ps*Toc34 GTPase

(A) Elution profile of a 1 mM mixture of GMP, GDP and GTP standards. Retention times are 3.8 min, 4.5 min and 5.6 min, respectively. (B) Elution of nucleotides from freshly purified *at*Toc33, showing a mixture of GDP and GTP loaded protein. (C) Elution profile of a 1 mM GMPPNP standard. The peak observed at 5 min originates from GMPPNP, while the peak at 4.0 min represents a known impurity resulting from of the production process (GMPPNP from Sigma Aldrich has a certified purity of > 85%). (D) Elution profile of GMPPPNP loaded *at*Toc33 using the nucleotide exchange protocol. GMPPNP is detectable as a single peak at 5 min retention time; the impurity observed with the GMPPNP standard in (C) at 4 min retention time is not seen in the GMPPNP exchanged protein sample. In all experiments a volume of 20 µl of injected on the column, the protein concentration was adjusted to 50 µM, the flow rate used was 1.0 ml/min.

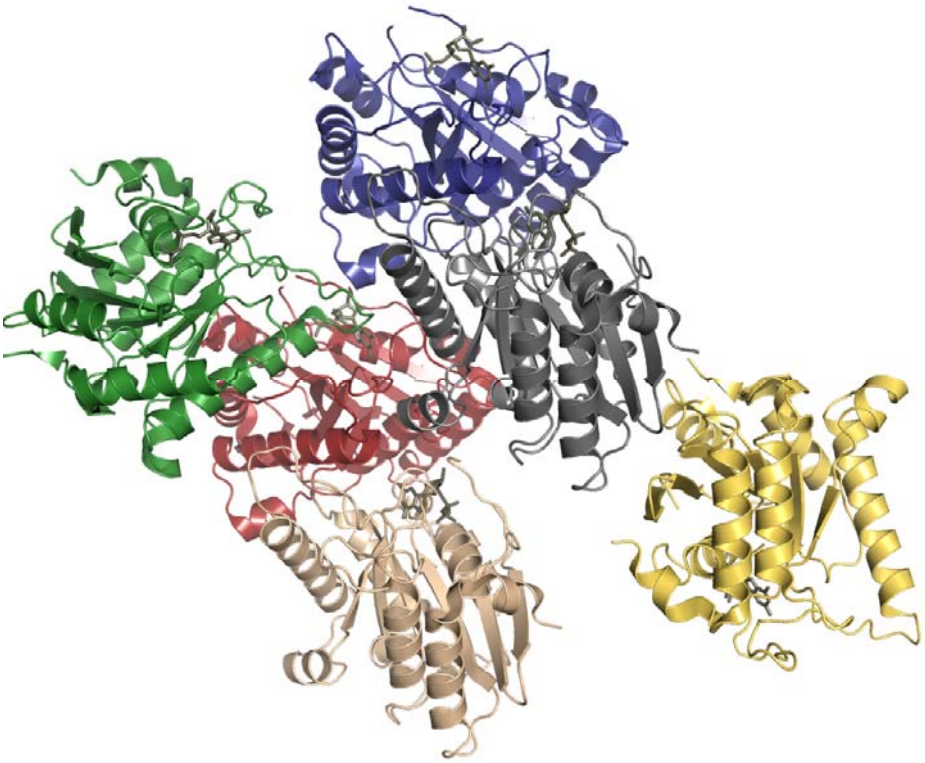

#	interacting monomer	symmetry operation	interface area [Å^2]
1	blue	-y+1/2,x+1/2,z+1/4	674.1
2	orange	y,x,-z	424.8
3	red	-y+1/2,x+1/2,z-3/4	328.5
4	brown	x,y,z-1	138.9
5	green	-x,-y+1,z-1/2	82.3

Figure S2. Analysis of Crystal Contacts
The table shows the relevant interfaces formed in the crystal between the grey monomer and neighbouring molecules, as calculated by the program PISA (Krissinel and Henrick, 2007). For comparison, the interface observed in the *ps*Toc34 dimer has a calculated interface area of 2750 Å^2.

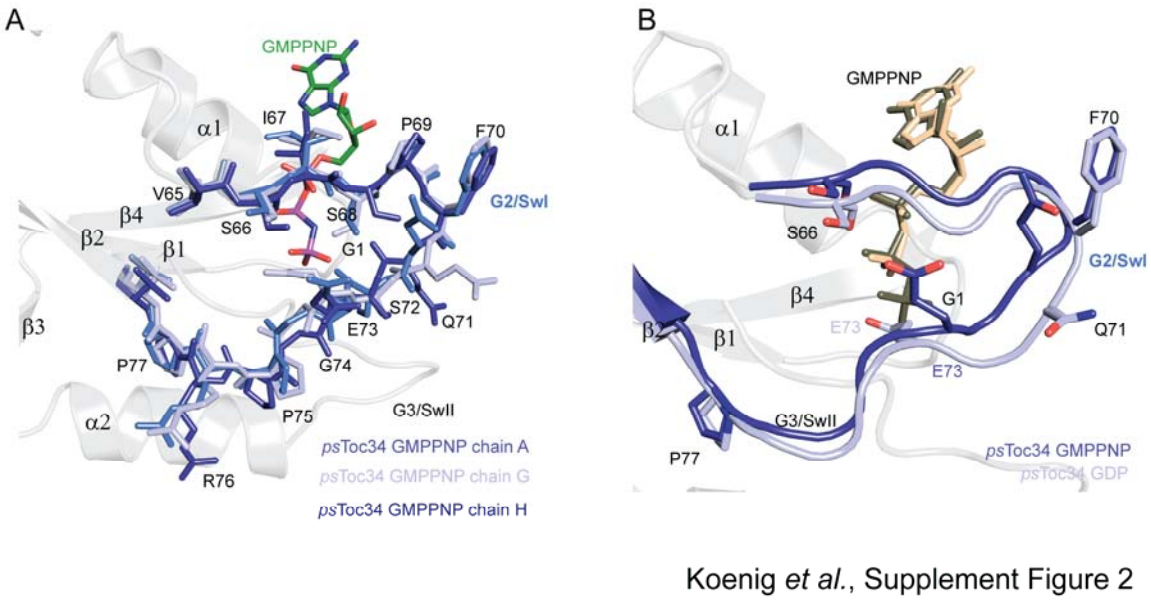

Figure S3. Disorder in the G2 / Switch I Element in Dimeric *ps*Toc34

(A) There are subtle changes in the G2 / switch I region, when the eight copies in the asymmetric unit are compared. The G2 / switch I region from Gln71 to Arg76 is somewhat flexible, though the conformational freedom is partly restricted by presence of the two prolines Pro69 and Pro75.

(B) Comparison of the G2 / switch I region between $Toc34_{GMPPNP}$ and $Toc34_{GDP}$. The main difference between GDP and GMPPNP states is positioning of Glu73 as discussed in the main text, this is the nucleotide *tracker* residue which monitors the nucleotide loading state.

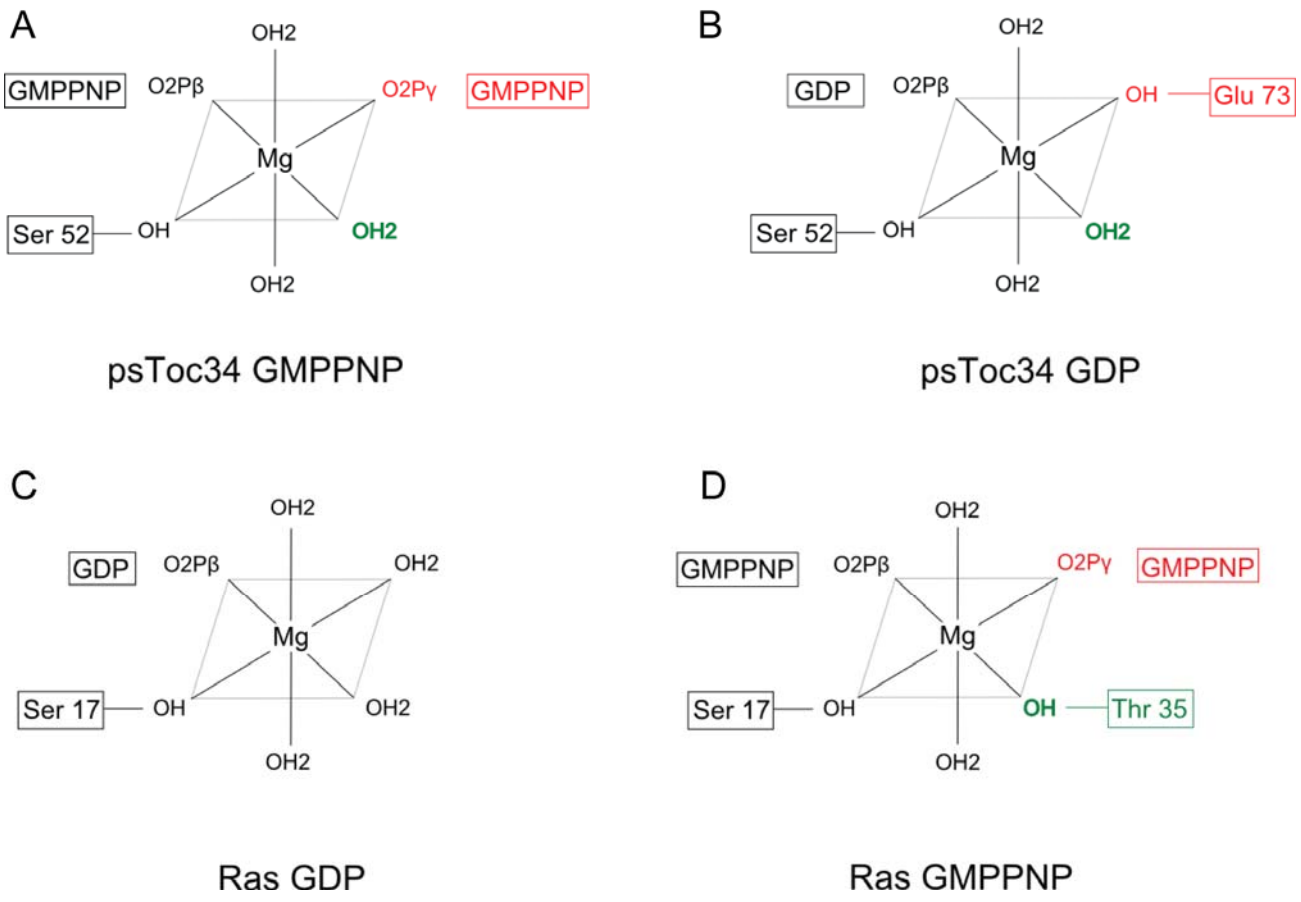

Figure S4. Mg^{2+} Coordination in *ps*Toc and p21 Ras

(A) Coordination of the magnesium-ion in the GMPPNP state of *ps*Toc34 by Ser52 from the G1 element, the β- and the γ-phosphate and three additional water molecules.

(B) Coordination of the magnesium-ion in the GDP state of *ps*Toc34 by Ser52 from the G1 element, Glu73 from the G2 element, the β-phosphate and three additional water molecules. Glu73 takes the coordination site of the γ-phosphate in $Toc34_{GMPPNP}$ as shown in (A)

(C) Coordination of the magnesium-ion in the GMPPNP state of p21 Ras. The magnesium-ion is coordinated by Ser17 from the G1 element, the β- and the γ-phosphate, a Thr from the G2 element, which is conserved among GTPases of the TRAFAC class and two additional water molecules.

(D) Coordination of the magnesium-ion in the GDP state of p21 Ras. The magnesium-ion is coordinated by Ser17 from the G1 element, the β-phosphate and three additional water molecules.

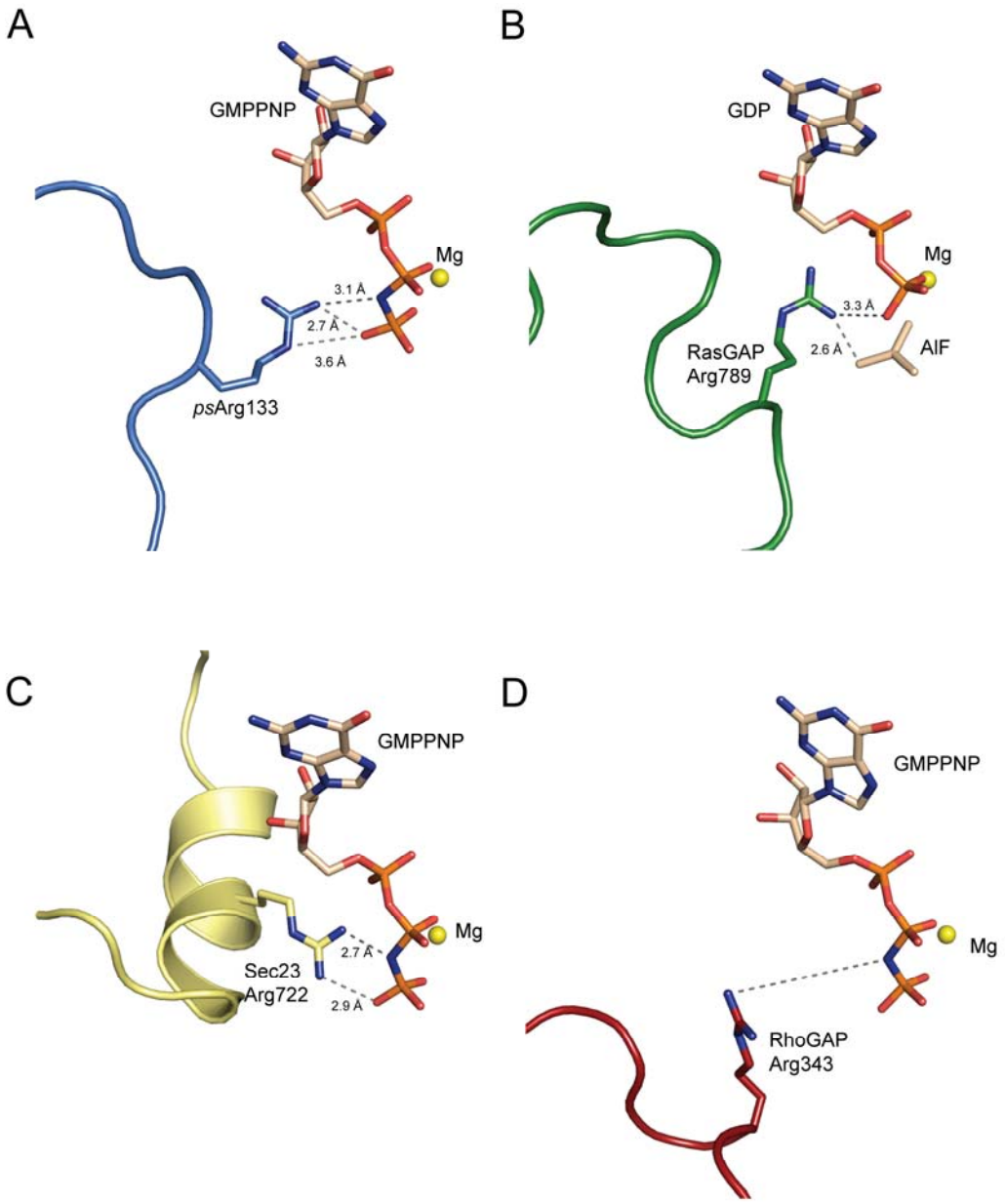

Figure S5. Comparison of *ps*Arg133 with Arginine Finger in different GTPase-GAP Complexes

(A) *ps*Toc34 CB-loop carring Arg133 inserted *in trans* in the nucleotide binding pocket of the dimerisation partner. (B) RasGAP-Ras argenine finger (PDB 1WQ1). A similar confirmation of arginine fingers is observed in the Cdc42:Cdc42GAP:GDP:AlF (PDB 1GRN) and in the Rho:RhoGAP:GDP:AlF (PDB 1TX4) structure. (C) Sec23:Sar1:GMPPNP arginine finger (PDB 1M2O). (D). Cdc42:RhoGAP GMPPNP arginine finger, which is turned away from the nucleotide and not in proper conformation for hydrolysis activation (PDB 1AM4).

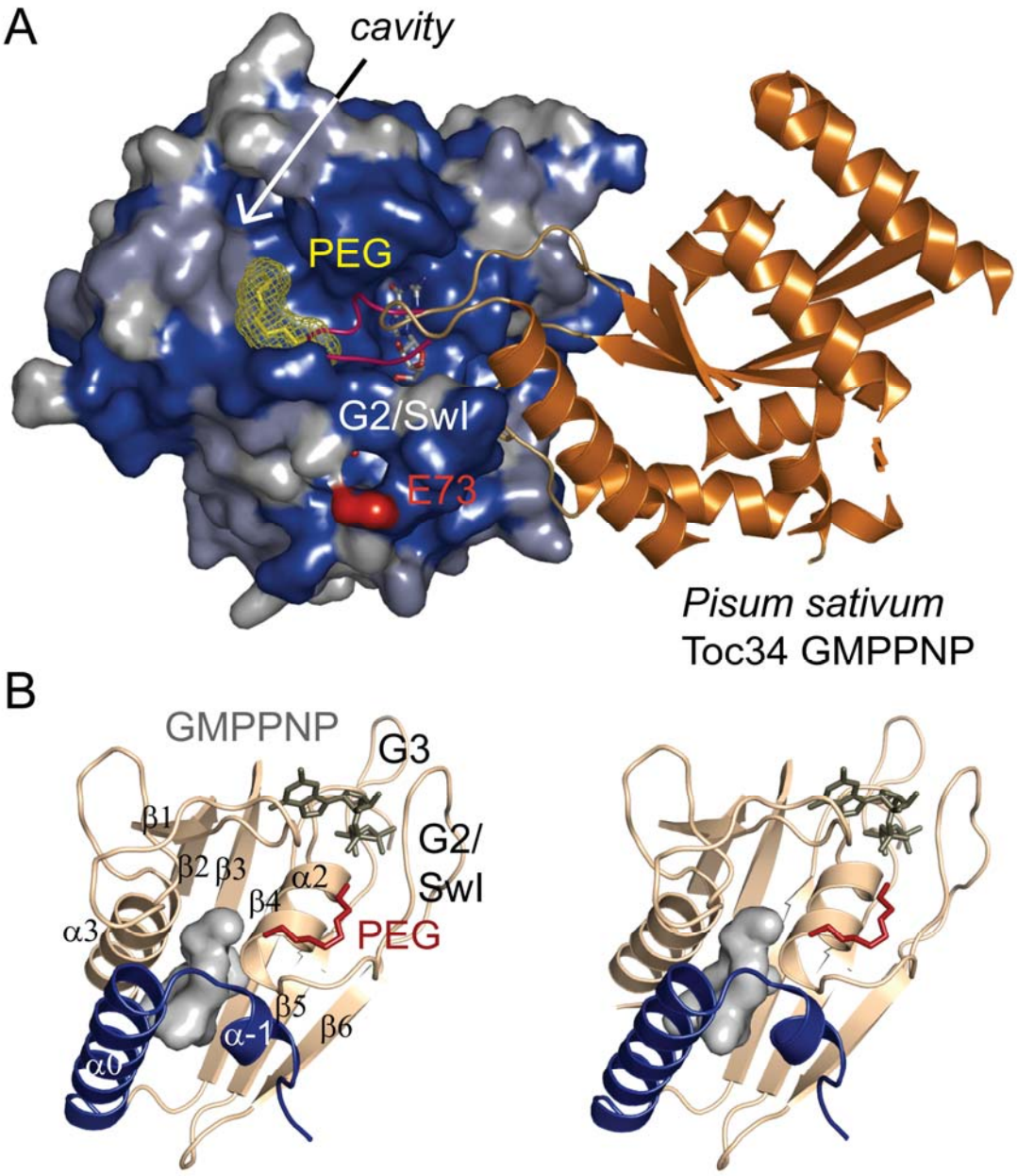

Figure S6. Binding Sites on Toc34

(A) Surface of Toc34 colored by the degree of conservation. Conservation is based on the alignment shown in Figure S7, using the program Consurf (Glaser et al., 2003). Dark colors show highly conserved residues, light colors variable regions. The regions around the potential binding site are highly conserved. Model of Toc159 as well as E73 compare Figure 6. (B) A PEG molecule is bound at a shallow cavity on the surface of *ps*Toc34. This molecule, originating from the crystallization conditions, binds close to the G2 elements and thus is in a suggestive position for an interaction that would occur in the Toc complex. Near the PEG binding site, there is a large cavity between helix α-1 and helix α0 and the central β-sheet of the GTPase domain. The cavity might be also part of the binding site.

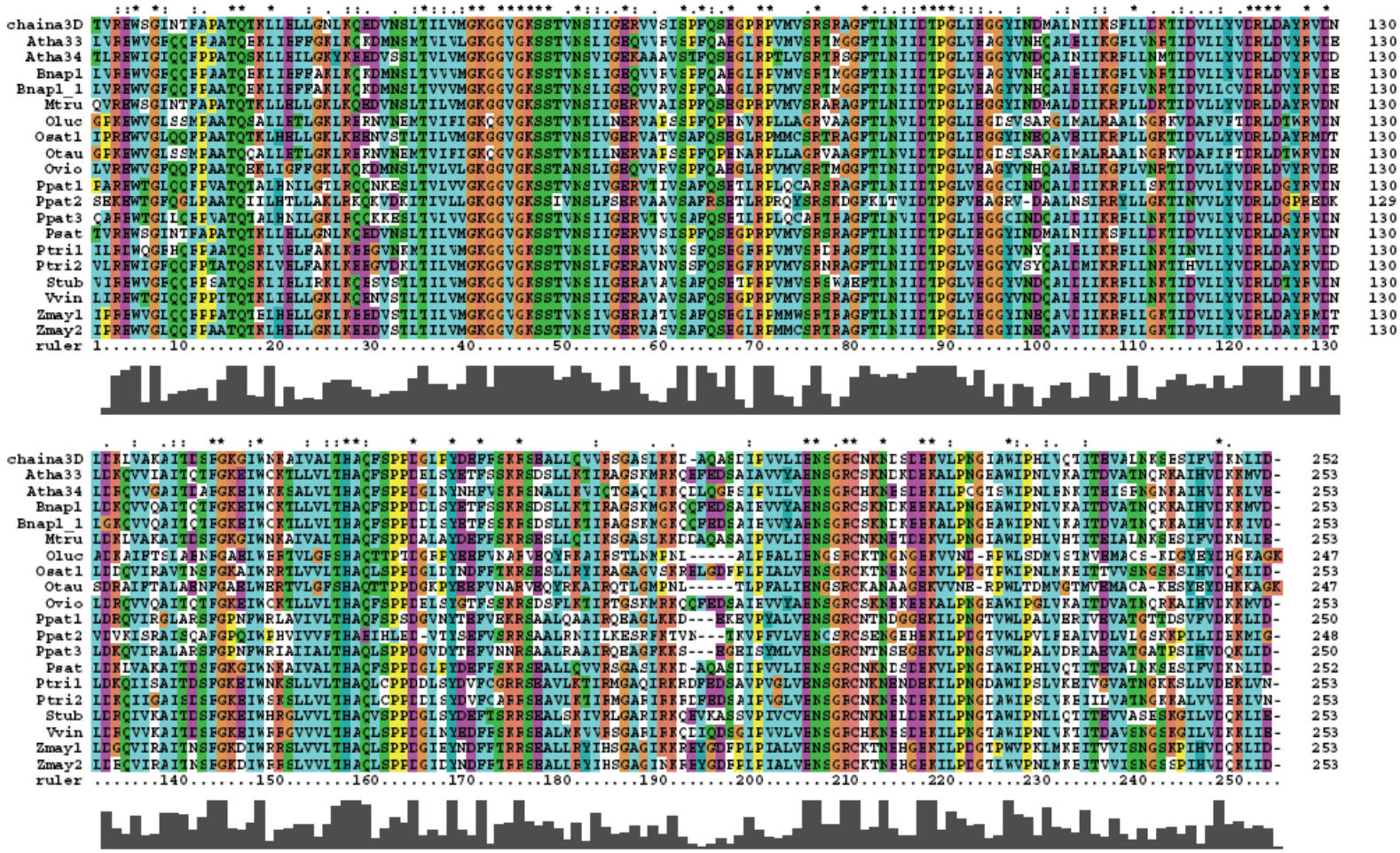

Figure S7. Alignment of Toc34 GTPases Used for Conservation Mapping as Shown in Figure S6

Prepared with ClustalX. The following proteins have been used in this alignment: Atha33: Toc33 from *Arabidopsis thaliana*, NP_171730; Atha34, Toc34 from *Arabidopsis thaliana*, NP_196119; Bnap1, Toc33 from *Brassica Nappus*, AAQ17548; Bnap1_1, TOC33-like protein from *Brassica Nappus*, AAQ73426; Mtru, Toc34 from *Medicago truncatula*, gb ABD28666.1; Oluc, predicted protein from *Ostreococcus lucimarinus CCE9901*, XP_001417009.1; Osat1, hypothetical protein OsJ_009702 from *Oryza sativa*, gb EAZ26219.1; Otau, Toc34 from *Ostreococcus tauri*, emb CAL53037.1; Ovio, Toc33-like protein from *Orychophragmus violaceus*, gb AAM77647.1; Ppat1, Toc34-1 from *Physcomitrella patens*, gb AAS47580.1; Ppat2, Toc34-2 from *Physcomitrella patens*, gb AAS47581.1; Ppat3, Toc34-3 from *Physcomitrella patens*, gb AAS47582.1; Psat, Toc34 from *Pisum sativum*, Q41009; Ptri1, protein from *Populus trichocarpa*, LG_XIV0229; Ptri2, protein from *Populus trichocarpa*, LG_II1667; Stub, GTP-binding-like protein from *Solanum tuberosum*, gb ABB16976.1; Vvin, hypothetical protein from *Vitis vinifera*, emb CAN63847.1; Zmay1, Toc34-1 protein from *Zea mays*, emb CAB65537.1; Zmay2, Toc34-2 protein from *Zea mays*, emb CAB77551.1.

Supplemental References

Glaser, F., Pupko, T., Paz, I., Bell, R.E., Bechor-Shental, D., Martz, E., and Ben-Tal, N. (2003). ConSurf: identification of functional regions in proteins by surface-mapping of phylogenetic information. Bioinformatics (Oxford, England) *19*, 163-164.

Krissinel, E., and Henrick, K. (2007). Inference of macromolecular assemblies from crystalline state. Journal of molecular biology *372*, 774-797.